



HAL
open science

Existence and stability of steady noncharacteristic solutions on a finite interval of full compressible Navier-Stokes equations

Blake Barker, Benjamin Melinand, Kevin Zumbrun

► **To cite this version:**

Blake Barker, Benjamin Melinand, Kevin Zumbrun. Existence and stability of steady noncharacteristic solutions on a finite interval of full compressible Navier-Stokes equations. 2019. hal-02352676v1

HAL Id: hal-02352676

<https://hal.science/hal-02352676v1>

Preprint submitted on 12 Nov 2019 (v1), last revised 12 Apr 2023 (v3)

HAL is a multi-disciplinary open access archive for the deposit and dissemination of scientific research documents, whether they are published or not. The documents may come from teaching and research institutions in France or abroad, or from public or private research centers.

L'archive ouverte pluridisciplinaire **HAL**, est destinée au dépôt et à la diffusion de documents scientifiques de niveau recherche, publiés ou non, émanant des établissements d'enseignement et de recherche français ou étrangers, des laboratoires publics ou privés.

Existence and stability of steady noncharacteristic solutions on a finite interval of full compressible Navier–Stokes equations

BLAKE BARKER* BENJAMIN MELINAND[†] AND KEVIN ZUMBRUN[‡]

November 12, 2019

Keywords: Steady solutions, gas dynamics, Evans function.

Abstract

We treat the 1D shock tube problem, establishing existence of steady solutions of full (nonisentropic) polytropic gas dynamics with arbitrary noncharacteristic data. We present also numerical experiments indicating uniqueness and time-asymptotic stability of such solutions. At the same time, we give an example of an (artificial) equation of state possessing a convex entropy for which there holds nonuniqueness of solutions. This is associated with instability and Hopf bifurcation to time-periodic solutions.

1 Introduction

In this paper, continuing investigation in [MZ19] of the isentropic case, we study by a combination of analytical and numerical techniques the existence, uniqueness, and stability of steady solutions of the full (nonisentropic) 1D compressible Navier–Stokes equations on a bounded interval, with noncharacteristic inflow-outflow boundary conditions.

This corresponds to the 1D version of the “shock tube” problem of describing flow in a finite length and width channel, with prescribed boundary conditions at the left and right ends. Our main interest is in large-amplitude data, since small-amplitude existence and uniqueness as we shall show, follow in 1D by straightforward entropy considerations.

As developed in the viscous shock case [BHZ10, BHLZ18a, BHLZ18b, HLZ09, HLZ17], a convenient method to study spectral stability is via numerical Evans function investigations. A useful necessary condition, also based on Evans function considerations, is the positivity of the stability index, a mod two count of the Morse index of the linearized operator about

*Brigham Young University, Provo, UT 84602; blake@mathematics.byu.edu: Research of B.B. was partially supported under NSF grant no. DMS-140087.

[†]CEREMADE, CNRS, Université Paris-Dauphine, Université PSL, 75016 PARIS, FRANCE; melinand@ceremade.dauphine.fr.

[‡]Indiana University, Bloomington, IN 47405; kzumbrun@indiana.edu: Research of K.Z. was partially supported under NSF grant no. DMS-1700279.

the wave. This was trivially evaluable in the isentropic case [MZ19], but is complicated in general. In particular, it does not seem to be analytically evaluable for the nonisentropic case considered here. It can be computed explicitly however in the “standing-shock limit” of [SZ01, Zum10], in which the steady solution is taken to be a sufficiently large piece of a standing viscous shock profile (see Appendix A.6).

1.1 Description of main results

Our main analytical results are (i) local uniqueness of almost constant steady solutions for general symmetrizable systems (Corollary A.6); (ii) global uniqueness of constant solutions for general systems with convex entropy (Theorem A.9); (iii) *global existence* of steady solutions of the full polytropic gas equations (2.1) (Corollary 4.5). We show, moreover, that global uniqueness of solutions of (2.1) is roughly equivalent to transversality of steady profiles as solutions of the ODE connection problem (2.6)-(2.10). This is equivalent to the nonvanishing of the Jacobian $\det(d\Psi)$ of (2.10) (Proposition 5.1).

Nonvanishing of $\det(d\Psi)$ is also seen to be equivalent to nonvanishing of the stability index (Lemma 6.1). Hence a change in sign implies appearance of both nonuniqueness and instability: the usual “exchange of stability” scenario familiar from finite-dimensional ODE. Thus we may study uniqueness in passing, in the course of a larger study of spectral stability.

Augmenting our analytical results for the full polytropic gas equations, we carry out such a study in Section 7 by a systematic numerical Evans function investigation of the “feasible set” \mathcal{C} of profiles realizable by numerical shootings. Our numerical findings (Section 7) are that, on the feasible set \mathcal{C} , the stability index is uniformly positive, indicating *uniqueness of large-amplitude solutions*, and that steady solutions exhibit *uniform spectral stability*. Finally, the nonlinear stability can be obtained by similar considerations to [MZ19, Section 6] (see also Remark A.8).

1.2 Discussion and open problems

The first local existence/uniqueness result for small-amplitude data has been established in [KK97]. We improved this result to large-amplitude data.

Our findings of global existence and uniqueness for the noncharacteristic problem parallel those of Lions [Lio98] in the characteristic case $u = 0$ on the boundary, for which he shows global existence and uniqueness of solutions for arbitrary prescribed average density, in 1- and multi-D. However, they are obtained by quite different techniques, which, moreover, are special to 1D. Indeed, though perhaps intuitively expectable, especially given the uniform shock stability results of [HLZ09, HLZ17] for the compressible Navier–Stokes equations, our results of large-amplitude existence, uniqueness and stability are obtained by a combination of exhaustive numerical investigations, and rather delicate degree-theoretic arguments specific to the equations of 1D polytropic gas dynamics under study.

In [SZ01, Zum10] the case of steady solutions on a half-line is investigated and it is shown that instability of steady solutions can occur, even for the most standard ideal polytropic gas

law. It suggests that the question of stability at least is not a foregone conclusion for steady solutions on the interval. Moreover, the nature of instability found in [SZ01, Zum10] involved change of sign in the stability index, which in the present case would signal nonuniqueness as well. On the other hand, our numerical findings (Section 7) indicate that neither of these phenomena in fact occur for polytropic gas dynamics on the interval.

This begs the question whether such detailed and special arguments are necessary, or whether there might instead exist some more straightforward argument for all or part of our results via general principles, such as, e.g., existence of convex entropy as used in Appendix A.4. We give a partial answer to this question in Section 8, exhibiting a counterexample involving an equation of state presented in [BFZ15] for which the equations of compressible gas dynamics possess a convex entropy, but global stability and uniqueness are violated. It is seen that the associated transition to instability can involve either steady bifurcation to multiple solutions, or *Hopf bifurcation to time-periodic solutions*. The latter phenomenon is significant as the first example of Hopf bifurcation for stationary solutions of compressible gas dynamics, similar to “galloping” or “cellular” instabilities in detonation [TZ11].

It is an interesting question whether our existence result extends to general equations of states considered in [BFZ15]. Note that we obtain nonuniqueness results for a particular equation of states in Section 8.

A further very interesting open problem is the extension of our existence results to the true multi-D shock tube problem, generalizing the small-amplitude existence-uniqueness results of [KK97], and the determination of stability of multi-D solutions even in the small-amplitude case.

Finally, another interesting open question is the rigorous characterization of structure in the small-viscosity limit. A preliminary, quite approachable, step in this direction would be to show existence and uniqueness of possible limiting configurations composed of shocks and boundary layers, as discussed at the end of Appendix A.5.2.

2 Preliminaries

2.1 Equations of motion

The 1D compressible Navier–Stokes equations in Eulerian coordinates are

$$(2.1) \quad \begin{aligned} \rho_t + (\rho u)_x &= 0, \\ (\rho u)_t + (\rho u^2 + p)_x &= \alpha u_{xx}, \\ (\rho E)_t + (\rho u E + pu)_x &= \kappa T_{xx} + (\alpha u u_x)_x \end{aligned}$$

where

$$E = e + \frac{u^2}{2}, \quad p = \Gamma \rho e, \quad e = c_v T,$$

with Γ , c_v , ν , and α fixed positive constants; see [Bat99, HLZ09, HLZ17]. We define $\nu = \frac{\kappa}{c_v}$.

Remark 2.1. For simple gases, the ratio $\frac{\nu}{\alpha}$ follows closely to the prediction

$$(2.2) \quad \frac{\nu}{\alpha} = \frac{27\Gamma + 12}{16}$$

of statistical mechanics [HLZ09, HLZ17].¹ In our numerics, we will assume, further, (2.2).

As described in [MZ19] in the isentropic case, we seek steady solutions on the interval $[0, 1]$, with noncharacteristic inflow-outflow boundary conditions

$$(2.3) \quad (\rho, u, e)(0) = (\rho_0, u_0, e_0), \quad (u, e)(1) = (u_1, e_1).$$

By changing ρ by $\rho_0\rho$, u by $\frac{1}{\rho_0}u$, t by ρ_0t and e by $\frac{1}{\rho_0}e$ (notice that we can not change x without changing the length of the interval), we assume in the following that

$$(2.4) \quad \rho_0 = 1, \quad u_0, e_0, u_1, e_1 > 0.$$

2.2 Profile equations and formulation as mapping problem

Our main interest is the study of steady solutions, i.e. solutions of

$$(2.5) \quad \begin{aligned} (\rho u)_x &= 0, \\ (\rho u^2 + \Gamma \rho e)_x &= \alpha u_{xx}, \\ \left(\rho u \left(e + \frac{u^2}{2} \right) + \Gamma \rho e u \right)_x &= \nu e_{xx} + (\alpha u u_x)_x. \end{aligned}$$

Integrating (2.5) from 0 to x and rearranging using (2.4), we obtain similarly as in [HLZ17] the profile ODE

$$(2.6) \quad \begin{aligned} \frac{\alpha}{u_0} u' &= c_1 + u + \Gamma \frac{e}{u}, \\ \frac{\nu}{u_0} e' &= c_2 - c_1 u - \frac{1}{2} u^2 + e, \end{aligned}$$

together with $\rho = \frac{u_0}{u}$, with the initial data

$$(2.7) \quad \begin{aligned} u(0) &= u_0 > 0 \\ e(0) &= e_0 > 0 \end{aligned}$$

and where $c = (c_1, c_2)$ are constants of integration to be determined. Indeed in our setting

$$(2.8) \quad c_1 = \frac{\alpha}{u_0} u'(0) - u_0 - \Gamma \frac{e_0}{u_0}, \quad c_2 = \frac{\nu}{u_0} e'(0) + \alpha u'(0) - e_0 - \frac{1}{2} u_0^2 - \Gamma e_0,$$

and we do not know the values of $(u'(0), e'(0))$.

¹In the notation of [HLZ17], $\alpha = 2\mu + \eta = \frac{4}{3}\mu$, $\gamma = \Gamma + 1$, and $\frac{\kappa}{c_v\mu} = \frac{9\gamma-5}{4}$, giving the result.

The domain of the ODE is the set

$$\{(u, e) \in \mathbb{R}^2, u > 0\}$$

so that the right hand side of (2.6) is well-defined and for which we can reconstruct ρ . Indeed, we remark that $u > 0$ is imposed by $\rho u = Cst$ and $\rho > 0$. Hence we may ignore the variable ρ in the following. Note also that the physical solutions are the one for which e is also positive.

For a fixed choice of left data (ρ_0, u_0, e_0) (meaning, by our previous normalization, just a fixed choice of u_0 and e_0), we define now the mapping

$$(2.9) \quad \Psi : (c_1, c_2) \rightarrow (u, e)(1),$$

where (u, e) denotes the maximal solution of (2.6)-(2.7) for the given value of $c = (c_1, c_2)$. Evidently, solutions of (2.3)-(2.5) thus correspond to solutions of the mapping problem

$$(2.10) \quad \Psi(c) = (u_1, e_1).$$

3 The feasible set

In (2.9), we did not specify the domain of c . It is indeed our first order of business to determine it. For a fixed choice of left data (u_0, e_0) , we define the feasible set \mathcal{C} as the set of all c for which (2.6)-(2.7) has a continuous solution (u, e) on $[0, 1]$ where u and e are both positive on $[0, 1]$. Note that \mathcal{C} is not empty since $(-u_0 - \Gamma \frac{e_0}{u_0}, -(1 + \Gamma)e_0 - \frac{1}{2}u_0^2) \in \mathcal{C}$ (that corresponds to a constant solution of problem (2.6)-(2.7)). Then, we have the following crucial observation.

Proposition 3.1. *The set \mathcal{C} is open and its boundary consists of c for which there exists continuous functions (u, e) on $[0, 1]$, solution of Problem (2.6)-(2.7) on $[0, 1)$, with u, e both positive on $[0, 1)$ and such that $e(1) = 0$.*

Before proving Proposition 3.1, we establish a preliminary result.

Lemma 3.2. *Let $c = (c_1, c_2) \in \mathbb{R}^2$. Let $x_* \in (0, 1]$ such that a solution (u, e) of (2.6)-(2.7) is defined on $[0, x_*)$. We have the following statements :*

(i) *If $e > 0$ on $[0, x_*)$, then (u, e) is bounded on $[0, x_*)$ uniformly with respect x_* and one can extend continuously (u, e) to x_* .*

(ii) *If there exists a constant $\tilde{e} > 0$, $e \geq \tilde{e} > 0$, then there exists a constant $\tilde{u} > 0$, $u > \tilde{u}$.*

(iii) *If $(u, e) \rightarrow 0$ simultaneously as $x \rightarrow x_*$ with (u, e) both positive, then $c_1 < 0$ and $c_2 < 0$.*

(iv) *Assume $c_1 < 0$, $c_2 < 0$, (u, e) is a solution of (2.6)-(2.7) on $[0, x_*]$ and $u, e > 0$ on $[0, x_*]$. For any $\varepsilon > 0$, there exists $\delta > 0$ depending only on c_1, c_2, ε such that if $u(x_*), e(x_*) \leq \delta$, there exists $\tilde{x} \in [x_*, x_* + \varepsilon]$ such that (u, e) extends continuously as a solution of (2.6)-(2.7) on $[0, \tilde{x})$ with $u, e > 0$ on $[0, \tilde{x})$ and $e(x) \rightarrow 0$ as $x \rightarrow \tilde{x}$.*

Remark 3.3. As we will see in the proof of (iv), one can prove that if $(c_1, c_2) \in \mathcal{C}$ with $c_1 < 0$, $c_2 < 0$ and (u, e) a solution of (2.6)-(2.7) on $[0, 1]$, there exists a constant $M > 0$ depending only on c_1, c_2, Γ , such that for any $\delta > 0$ small enough, for any $x_* \in (0, 1)$, if $0 < u(x_*), e(x_*) \leq \delta$, then $0 < e \leq \delta$ and $0 < u \leq M\delta$ on $[x_*, 1]$.

Proof. (i) Since $e > 0$ on $[0, x_*)$, we get

$$\begin{aligned} \frac{1}{2} \left(\frac{\alpha}{u_0} u^2 + \frac{\nu}{u_0} e^2 \right)' &= c_1 u + u^2 + \Gamma e + c_2 e - c_1 e u - e u^2 / 2 + e^2 \\ &\leq c_1 u + u^2 + \Gamma e + c_2 e - c_1 e u + e^2 \\ &\leq A \left(\frac{\alpha}{u_0} u^2 + \frac{\nu}{u_0} e^2 \right) + B \end{aligned}$$

for some constants $A, B > 0$ depending on $c_1, c_2, \Gamma, \alpha, \nu, u_0$. Hence, $|(u, e)|$ grows at most exponentially, in particular remaining bounded on $[0, x_*)$. Furthermore, u and e can be continuously extended to x_* since $(u^2)'$ and $(e^2)'$ are bounded and then integrable on $[0, x_*)$.

(ii) This statement is clear since the term $\Gamma \frac{e}{u}$ in the u -equation serves as a barrier.

(iii) Evidently, $c_1 < 0$, or else $u' > 0$ for $u, e > 0$, contradicting the assumed convergence to 0. Then, for $u > 0$ sufficiently small, this implies that $-c_1 u - \frac{1}{2} u^2 > 0$ and hence $\frac{\nu}{u_0} e' > c_2 + e$. Therefore, $c_2 < 0$ or else $e' > 0$ for $e > 0$ and $u > 0$ sufficiently small, again contradicting convergence. This proves the first assertion.

(iv) We assume now that $c_1, c_2 < 0$, that (u, e) are both positive on $[0, x_*]$ and that $u(x_*), e(x_*) \leq \delta$. We first note that so long as $u, e < \frac{c_2}{c_1 - 1}$, $\frac{\nu}{u_0} e' < -\frac{1}{2} u^2 \leq 0$ and e is decreasing. Next if δ is small enough, based on the u -equation, several situations can happen:

- (a) If $u(x_*) > \frac{-c_1 - \sqrt{c_1^2 - 4\Gamma e(x_*)}}{2}$, $u'(x_*) < 0$ and u is decreasing about x_* .
- (b) If $u(x_*) = \frac{-c_1 - \sqrt{c_1^2 - 4\Gamma e(x_*)}}{2}$, $u'(x_*) = 0$, $u''(x_*) = \Gamma \frac{e'(x_*)}{u(x_*)} < 0$, u is decreasing about x_* .
- (c) If $u(x_*) < \frac{-c_1 - \sqrt{c_1^2 - 4\Gamma e(x_*)}}{2}$, $u'(x_*) > 0$ and $u < \frac{-c_1 - \sqrt{c_1^2 - 4\Gamma e}}{2} \leq 2\Gamma \frac{|e|}{|c_1|}$ about x_* .

Therefore, for δ small enough, $u \leq \max\left(1, \frac{2\Gamma}{|c_1|}\right) \delta$ and $\frac{\nu}{u_0} e' < \frac{c_2}{2}$ so long as $0 \leq e \leq \delta$. Hence e goes to zero at \tilde{x} for $|\tilde{x} - x_*| \leq \frac{2\nu}{u_0 |c_2|} \delta$. This proves assertion (iv). \square

Thanks to this lemma we can assert that

$$\mathcal{C} = \{c \in \mathbb{R}^2, \text{ where } e > 0 \text{ on } [0, 1], (u, e) \text{ the maximal solution of (2.6)-(2.7)}\}.$$

Proof of Proposition 3.1. For $c = (c_1, c_2)$, we denote by (u, e) the maximal solution of Problem (2.6)-(2.7). Note that the following map is locally Lipschitz

$$(3.1) \quad \Phi : (u, e) \in \{(u, e) \in \mathbb{R}^2, u > 0\} \mapsto \left(c_1 + u + \frac{\Gamma e}{u}, c_2 - c_1 u - \frac{1}{2} u^2 + e \right).$$

If $c \in \mathcal{C}$, then u and e are defined and positive on $[0, 1]$ and by continuous dependence on parameters of solutions of an ODE, c lies in the interior of \mathcal{C} . In particular \mathcal{C} is open.

We assume in the following that $c \in \mathcal{C}^c$. Thanks to Lemma 3.2(i)-(ii), there exists $x_* \in (0, 1]$ such that u and e are defined and continuous on $[0, x_*)$, $u, e > 0$ on $[0, x_*)$ and (u, e) can be extended to x_* with $e(x_*) = 0$ and $u(x_*) \geq 0$. Three different situations can then occur.

Case (i) : $x_* = 1$ and then $e(1) = 0$.

Case (ii) : $u(x_*) > 0$ and $x_* < 1$. Then (u, e) is defined on a interval that strictly contains $[0, x_*]$ and $e'(x_*) \leq 0$. If $e'(x_*) < 0$, e must actually cross 0 and must become negative as x crosses x_* . On the other hand if $e'(x_*) = 0$

$$\frac{\nu}{u_0} e''(x_*) = -(c_1 + u(x_*))u'(x_*) = -\frac{u_0}{\alpha} (c_1 + u(x_*))^2$$

and e crosses 0 unless $u(x_*) = -c_1$ and simultaneously $u'(x_*) = 0$. But, then, repeated differentiation shows that, if $u(x_*) = -c_1$, $e(x_*) = 0$ and $e'(x_*) = 0$, derivatives of e and u at x_* vanish to all orders. By analyticity of solutions of an analytic ODE (note that $u > 0$), $e \equiv 0$ and $u \equiv -c_1$, contradicting $e(0) > 0$.

Therefore in any cases, there exists $\varepsilon > 0$ small enough such that (u, e) is defined on $[0, x_* + \varepsilon]$, e negative on $]x_*, x_* + \varepsilon]$ and u positive on $[0, x_* + \varepsilon]$. By continuous dependence on parameters, c lies in the interior of \mathcal{C}^c . In particular $c \notin \partial\mathcal{C}$.

Case (iii) : $u(x_*) = 0$ and $x_* < 1$. In this case, Lemma 3.2(iii) shows that $c_1, c_2 < 0$. Let $(\tilde{c}_1, \tilde{c}_2)$ close enough to (c_1, c_2) and denote by (\tilde{u}, \tilde{e}) the maximal solution of Problem (2.6)-(2.7) associated to $(\tilde{c}_1, \tilde{c}_2)$. We then take a δ associated to $\varepsilon = 1 - x_*$ in Lemma 3.2(iv) that works for any $(\tilde{c}_1, \tilde{c}_2)$ close enough to (c_1, c_2) . By continuity of u and e , there exists a number $\mu > 0$ small enough such that $0 < u(x_* - \mu), e(x_* - \mu) \leq \frac{\delta}{2}$. Then, by continuous dependence on parameters, for any $(\tilde{c}_1, \tilde{c}_2)$ close enough to (c_1, c_2) , (\tilde{u}, \tilde{e}) is defined on $[0, x_* - \mu]$ and $0 < \tilde{u}(x_* - \mu), \tilde{e}(x_* - \mu) \leq \delta$. Lemma 3.2(iv) shows that there exists $\tilde{x} \in [x_* - \mu, 1 - \mu]$, $\tilde{e}(\tilde{x}) = 0$. In particular, $c \notin \partial\mathcal{C}$. \square

We can now show that Ψ defined in (2.9) is continuous.

Proposition 3.4. *The map Ψ is continuous on \mathcal{C} and can be extended to $\bar{\mathcal{C}}$ as a continuous map denoted again Ψ .*

Proof. The fact that Ψ is continuous on \mathcal{C} follows from continuous dependence on parameters of solutions of an ODE (and the fact that the map Φ defined in (3.1) is locally Lipschitz). We consider now $c = (c_1, c_2) \in \partial\mathcal{C}$. Proposition 3.1 shows the maximal solution (u, e) of (2.6)-(2.7) is defined and continuous on $[0, 1]$ and can be extended continuously to 1 with $e(1) = 0$ and $u(1) \geq 0$. Therefore, we can define $\Psi(c) = (u(1), 0)$. If $u(1) > 0$, (u, e) is defined on a interval that strictly contains $[0, 1]$ and by continuous dependence on parameters, Ψ is continuous at c . We know have to deal with the case $u(1) = 0$. Lemma 3.2(iii) shows that $c_1, c_2 < 0$. Consider $\varepsilon > 0$. Let $\tilde{c} \in \mathcal{C}$ close enough to c and denote by (\tilde{u}, \tilde{e}) the maximal solution of Problem (2.6)-(2.7) associated to \tilde{c} . By continuity of (u, e) there exists $x_* \in (0, 1)$ such that $0 < u(x_*), e(x_*) \leq \frac{\varepsilon}{2}$. Then, by continuous dependence on parameters, for any \tilde{c} close enough to c , we have $0 < \tilde{u}(x_*), \tilde{e}(x_*) \leq \varepsilon$. Finally, since $\tilde{c} \in \mathcal{C}$,

by taking ε small enough, Remark 3.3 gives $0 < \tilde{u}(1) \leq M\varepsilon$ (where M depends only on c and Γ). Hence, Ψ is continuous at c . \square

4 Existence

We are now ready to study existence. We first show that Ψ is “proper” in the following sense.

Proposition 4.1. *Assume that $u_0 > 0, e_0 > 0$ are fixed. Let $c = (c_1, c_2) \in \mathbb{R}^2$, such that $|c| \gg 1$ and denote by (u, e) the maximal solution of (2.6)-(2.7). Then, if $c \in \mathcal{C}$, either $u(1) \gg 1, e(1) \gg 1$ or $0 < u(1) \ll 1$.*

Proof. Several situations can happen.

Case (i) ($c_1 \gg 1$). If $c \in \mathcal{C}$, $\frac{\alpha}{u_0}u' \geq c_1 + u_0$ and $u(1) \geq \frac{u_0}{\alpha}(c_1 + u_0) + u_0 \gg 1$.

Case (ii) ($c_2 \ll -1$). We consider the energy $y = \frac{\alpha}{2u_0}u^2 + \frac{\nu}{u_0}e$. Then,

$$y' = c_2 + (\Gamma + 1)e + \frac{u^2}{2} \leq c_2 + My$$

where M is a constant depending only on Γ, u_0, α, ν . Therefore, there exists a constant $A > 0$ depending only on $u_0, e_0, \alpha, \nu, \Gamma$ such that for any $c_2 \leq -A, c \notin \mathcal{C}$.

Case (iii) ($c_2 \gg 1$). Let $c \in \mathcal{C}$. We consider again the energy $y = \frac{\alpha}{2u_0}u^2 + \frac{\nu}{u_0}e$. Then,

$$y' = c_2 + (\Gamma + 1)e + \frac{u^2}{2} \geq c_2 + my$$

where m is a constant depending only on Γ, u_0, α, ν . Therefore either $e(1) \gg 1$ or $u(1) \gg 1$.

Case (iv) ($c_1 \ll -1$ and $c_2 \leq A$, for A sufficiently large) Let $c \in \mathcal{C}$. Using again $y = \frac{\alpha}{2u_0}u^2 + \frac{\nu}{u_0}e$ and following case (ii), we get $y' \leq A + My$. In particular, since $c_1 \ll -1$, there exists a constant B depending only on $u_0, e_0, \alpha, \nu, \Gamma, A$ such that $e \leq B$ on $[0, 1]$. Using this fact on the u-equation of System (2.6), we get

$$\frac{\alpha}{u_0}u' \leq c_1 + u + \frac{\Gamma B}{u}.$$

Noticing that $\frac{\alpha}{u_0}u' \leq \frac{1}{2}c_1$ for $u \in \left[-\frac{c_1}{4} - \frac{1}{2}\sqrt{\frac{1}{4}c_1^2 - 4\Gamma B}, -\frac{c_1}{4} + \frac{1}{2}\sqrt{\frac{1}{4}c_1^2 - 4\Gamma B}\right]$, we obtain that $u(1) \leq -\frac{c_1}{4} - \frac{1}{2}\sqrt{\frac{1}{4}c_1^2 - 4\Gamma B} \leq \frac{4\Gamma B}{|c_1|}$ and $u(1) \ll 1$. \square

Remark 4.2. *We proved in the previous proposition that there exists a constant $A > 0$ depending only on $u_0, e_0, \alpha, \nu, \Gamma$ such that for any $c_2 \leq -A, c \notin \mathcal{C}$ (see case(ii)). Note also that if $\frac{\nu}{u_0}e_0 + c_2 - c_1u_0 - \frac{1}{2}u_0^2 + e_0 \leq 0$ and $c_1 + u_0 \geq 0$, then $c \notin \mathcal{C}$. Indeed, in this case, u increases and $-c_1u - \frac{1}{2}u^2 \leq -c_1u_0 - \frac{1}{2}u_0^2$ so that e is decreasing, $e' \leq -e_0$ and then e crosses 0 in $(0, 1]$.*

The previous proposition is not empty in the sense that \mathcal{C} is not bounded.

Lemma 4.3. *Assume $u_0 > 0, e_0 > 0$ are fixed. There exists a positive number A depending only on $\Gamma, u_0, e_0, \alpha, \nu$ such that if $c_1 + u_0 + \frac{\Gamma A(|c_2|+1)}{u_0} < 0$ and $c_2 + e_0 > 0$, then $(c_1, c_2) \in \mathcal{C}$.*

Proof. For $c = (c_1, c_2)$, we denote by (u, e) the maximal solution of Problem (2.6)-(2.7) and by I its interval of definition. Following case (ii) in the previous proposition there exists a constant $A > 0$ depending only on $\Gamma, u_0, e_0, \alpha, \nu$ such that $e \leq A(|c_2| + 1)$ on $[0, 1] \cap I$. Then, we saw that so long as $0 \leq u \leq u_0$,

$$\frac{\alpha}{u_0} u' \leq c_1 + u + \Gamma \frac{A(|c_2| + 1)}{u} \quad \text{and} \quad \frac{\nu}{u_0} e' \geq c_2 + e.$$

Since $u'(0) < 0$ and $e'(0) > 0$ we get from Lemma 3.2(i)-(ii) that $[0, 1] \subset I$, e is increasing and $0 < u \leq u_0$ on $[0, 1]$. In particular $c \in \mathcal{C}$. \square

We now define for $\varepsilon > 0$, $E_\varepsilon = \{(x, y) \in \mathbb{R}^2, \varepsilon < x, y < \frac{1}{\varepsilon}\}$ and $\Omega_\varepsilon = \Psi^{-1}(E_\varepsilon)$. By continuity of Ψ (Proposition 3.4) and Proposition 4.1, Ω_ε is open, bounded and $\overline{\Omega_\varepsilon} \subset \mathcal{C}$. We denote Ψ_ε as the restriction of Ψ to Ω_ε .

Corollary 4.4. *Assume that $u_0 > 0$ and $e_0 > 0$ are fixed. Let $u_1 > 0, e_1 > 0$. Then for $\varepsilon > 0$ small enough, $(u_1, e_1) \notin \Psi(\partial\Omega_\varepsilon)$ and the Brouwer degree $d(\Psi_\varepsilon, \Omega_\varepsilon, (e_1, u_1))$ is independent of (u_1, e_1) and ε .*

Proof. Let $u_1 > 0, e_1 > 0$. First, Proposition 4.1 shows that $\Psi^{-1}(u_1, e_1)$ is bounded and included in the open set Ω_ε for ε small enough. In particular, $d(\Psi_\varepsilon, \Omega_\varepsilon, (e_1, u_1))$ is independent of ε small enough. Furthermore, we also get from Proposition 4.1 that for any $t \in [0, 1]$, $(1 + (1 - t)u_1, 1 + (1 - t)e_1) \notin \Psi(\partial\Omega_\varepsilon)$ if ε is small enough. Hence, by homotopy invariance, $d(\Psi_\varepsilon, \Omega_\varepsilon, (e_1, u_1))$ and $d(\Psi_\varepsilon, \Omega_\varepsilon, (1, 1))$ are equal. \square

Corollary 4.5 (Large-data existence). *There is at least one steady solution for every choice of left and right data.*

Proof. Applying Corollary 4.4, we find that the Brouwer degree is independent of the target (u_1, e_1) . Thus we may compute the degree at the constant data $(u_1, e_1) = (u_0, e_0)$. But, by Theorem A.9, constant solutions of general systems possessing a convex entropy are globally unique and nondegenerate in the sense that $\det(d\Psi(-u_0 - \Gamma \frac{e_0}{u_0}, -(1 + \Gamma)e_0 - \frac{1}{2}u_0^2)) \neq 0$ (indeed, we may check by direct computation the map Ψ is full rank at the corresponding value), and thus the degree for constant data is ± 1 .² But this implies that the Brouwer degree is ± 1 for all values of the target. Since degree is 0 in a domain without any roots, this implies in standard fashion that there exists at least one solution for any choices of target (u_1, e_1) . \square

²Here, we are using the standard fact that (2.5) possesses a convex entropy [Lax73, Smo94].

5 Uniqueness

Proposition 5.1. *If $\gamma := \det(d\Psi(c))$ does not vanish on the feasible set \mathcal{C} , then solutions of (2.10) are globally unique for each choice of data $(\rho_0, u_0, e_0, u_1, e_1)$. If on the other hand γ changes sign on the feasible set \mathcal{C} , then even local uniqueness is violated; in particular, there is at least one choice of data possessing multiple solutions.*

Proof. Nonvanishing of γ implies nonvanishing of the Jacobian determinant $\det(d\Psi(c))$, which implies constant sign and full rank at all points c . It follows that the degree of Ψ with respect to a target (u_1, e_1) is exactly equal to the (constant) sign of γ times n , where n is the number of solutions for that data. Since we have already shown that degree is identically equal to ± 1 , this is a contradiction unless roots are unique i.e., $n = 1$. This proves the first assertion. For the second assertion, just notice that uniqueness implies that degree is equal to the sign of γ at the unique solution and therefore a change of sign in γ implies a change in degree hence by contradiction uniqueness is impossible when γ changes sign. \square

Conclusion: *Uniqueness or nonuniqueness hinges on nonvanishing of $\det(d\Psi(\cdot))$ on \mathcal{C} .*

6 Spectral stability and the Evans function

We can reduce Problem (2.1) to

$$\begin{aligned}\rho_t + (\rho u)_x &= 0, \\ \rho u_t + \rho u u_x + (\Gamma \rho e)_x &= \alpha u_{xx}, \\ \rho e_t + \rho u e_x + \Gamma \rho e u_x &= \nu e_{xx} + \alpha u_x^2,\end{aligned}$$

from which we obtain the eigenvalue problem about a steady state $(\hat{\rho}, \hat{u}, \hat{e})$

$$(6.1) \quad \begin{aligned}\lambda \rho + (\hat{\rho} u + \hat{u} \rho)_x &= 0, \\ \lambda \hat{\rho} u + (\hat{\rho} \hat{u} u + \Gamma \hat{\rho} e + \Gamma \hat{e} \rho)_x + \hat{u}_x (\hat{\rho} u + \hat{u} \rho) &= \alpha u_{xx}, \\ \lambda \hat{\rho} e + (\hat{\rho} \hat{u} e)_x + \hat{e}_x (\hat{\rho} u + \hat{u} \rho) + \Gamma \hat{\rho} \hat{e} u_x + \Gamma \hat{u}_x (\hat{\rho} e + \hat{e} \rho) &= \nu e_{xx} + 2\alpha \hat{u}_x u_x,\end{aligned}$$

with boundary conditions

$$(6.2) \quad (\rho, u, e)(0) = 0, \quad (u, e)(1) = 0.$$

Note that for $\lambda = 0$ the previous system can be written in the alternative form

$$(6.3) \quad \begin{aligned}\hat{\rho} u + \hat{u} \rho &= 0, \\ (\hat{\rho} \hat{u} u + \Gamma \hat{\rho} e + \Gamma \hat{e} \rho)_x &= \alpha u_{xx}, \\ ((1 + \Gamma) \hat{\rho} \hat{u} e + \hat{\rho} \hat{u}^2 u)_x &= \nu e_{xx} + \alpha (\hat{u} u_x + \hat{u}_x u)_x.\end{aligned}$$

The *Evans function* [Rou01, SZ01] is defined as³

$$(6.4) \quad D(\lambda) := \det \begin{pmatrix} u_1(1) & u_2(1) \\ e_1(1) & e_2(1) \end{pmatrix},$$

where (ρ_j, u_j, e_j) are solutions of (6.1) with initial conditions

$$(\rho_1, u_1, e_1, u'_1, e'_1)(0) = (0, 0, 0, 1, 0), \quad (\rho_2, u_2, e_2, u'_2, e'_2)(0) = (0, 0, 0, 0, 1).$$

Evidently, $D(\cdot)$ is analytic in λ on all of \mathbb{C} , and real-valued for λ in \mathbb{R} , with zeros corresponding to eigenvalues of the linearized operator about the associated steady solution.⁴

Conclusion: *Spectral stability is equivalent to nonvanishing of D on $\{\Re\lambda \geq 0\}$.*

6.1 The stability index

It is readily seen (see, e.g. [MZ19]) that $D(\lambda) \neq 0$ for λ real and sufficiently large, hence we may define as in [GZ98] the *Stability index*

$$\mu := \operatorname{sgn} D(0) \left(\lim_{\lambda \rightarrow +\infty_{\text{real}}} \operatorname{sgn} D(\lambda) \right)$$

as a nonvanishing multiple $\pm \operatorname{sgn} D(0)$ of $\operatorname{sgn} D(0)$. Evidently, μ determines the parity of the number of roots of the Evans function with positive real part, or, equivalently (since complex roots occur in conjugate pairs), the number of positive real roots, with $+1$ corresponding to “even” and -1 to “odd”. As such, it is often useful in obtaining *instability* information.

Moreover, we have the following key observation relating the low-frequency stability and the stability index information to transversality of the steady profile solution of the standing-wave ODE.

Lemma 6.1. *The zero-frequency limit $D(0)$ is equal to $\frac{\alpha\nu}{u_0^2}$ multiplied by the Jacobian determinant $\det(d\Psi(c))$ associated with problem (2.10) evaluated at root c .*

Proof. The proof amounts to the observation that the operations of linearization and integration of the standing-wave ODE commute. Taking the variation of the profile equation (2.6) with respect to c gives

$$(6.5) \quad \begin{aligned} \frac{\alpha}{u_0} \dot{u}' &= \dot{c}_1 + \dot{u} + \Gamma \left(\frac{\dot{e}}{\hat{u}} - \frac{\hat{e}}{\hat{u}^2} \dot{u} \right), \\ \frac{\nu}{u_0} \dot{e}' &= \dot{c}_2 - (\dot{c}_1 \hat{u} + c_1 \dot{u}) - \hat{u} \dot{u} + \dot{e}, \\ (\dot{u}, \dot{e})(0) &= (0, 0), \end{aligned}$$

³We are using here the standard approach [AGJ90, GZ98] of rewriting (6.1) as a first-order system and a Cauchy problem

⁴Indeed, as standard in Evans function theory, zeros correspond in both location and multiplicity to eigenvalues of the linearized operator about the wave; see, e.g., [AGJ90, GZ98, ZH02] in the whole-line case.

where $\dot{\cdot}$ denotes variation. Furthermore, we deduce from relations (2.8) that

$$(\dot{c}_1, \dot{c}_2) = \left(\frac{\alpha}{u_0} \dot{u}'(0), \frac{\nu}{u_0} \dot{e}'(0) + \alpha \dot{u}'(0) \right).$$

It is readily verified for $\lambda = 0$ that the eigenvalue equations (6.3) can be integrated from 0 to x to yield the same system (6.5) (note that $\hat{\rho}\hat{u} = u_0$). Therefore, keeping the notations of (6.4), for $(\dot{c}_1, \dot{c}_2) = (1, 0)$, $(\dot{u}, \dot{e}) = \frac{u_0}{\alpha}(u_1, e_1) - \frac{u_0^2}{\nu}(u_2, e_2)$, whereas for $(\dot{c}_1, \dot{c}_2) = (0, 1)$, $(\dot{u}, \dot{e}) = \frac{u_0}{\nu}(u_2, e_2)$. The result follows. \square

Remark 6.2. *The previous lemma gives us another way to compute $D(0)$. Considering the problem*

$$(6.6) \quad \begin{aligned} \frac{\alpha}{u_0} u' &= d_1 + \left(1 - \Gamma \frac{\hat{e}}{\hat{u}^2}\right) u + \frac{\Gamma}{\hat{u}} e, \\ \frac{\nu}{u_0} e' &= d_2 - d_1 \hat{u} - \frac{\alpha}{u_0} \hat{u}' u + e + \Gamma \frac{\hat{e}}{\hat{u}} u, \\ u(0) &= 0, e(0) = 0, \end{aligned}$$

we have

$$D(0) = \det \begin{pmatrix} u_1(1) & u_2(1) \\ e_1(1) & e_2(1) \end{pmatrix}$$

where (u_1, e_1) solves (6.6) for $(d_1, d_2) = \left(\frac{\alpha}{u_0} - u_0 - \Gamma \frac{e_0}{u_0}, \alpha - e_0 - \frac{1}{2}u_0^2 - \Gamma e_0\right)$ and (u_2, e_2) solves (6.6) for $(d_1, d_2) = \left(-u_0 - \Gamma \frac{e_0}{u_0}, \frac{\nu}{u_0} - e_0 - \frac{1}{2}u_0^2 - \Gamma e_0\right)$ (see (2.8) for the link between (c_1, c_2) and $(u'(0), e'(0))$).

Remark 6.3. *Lemma 6.1 is analogous to the Zumbrun-Serre/Rousset lemmas of [ZS99, Rou01] in the whole- and half-line case, which say $D(\lambda) \sim \gamma \delta(\lambda)$ for $|\lambda| \ll 1$, where γ is a Wronskian encoding transversality of the associated standing-wave ODE and δ is a Lopatinski determinant for the inviscid stability problem (here trivially nonvanishing).*

Conclusion: Both Brouwer degree $\gamma = \text{sgn}(\det d\Psi)$ and stability index μ are determined by $\text{sgn}(D(0))$, hence (by Proposition 5.1 and the discussion just above) uniqueness and topological stability information may be obtained by evaluation of $D(0)$ on the feasible set \mathcal{C} . In particular, differently from the cases of the whole- or half-line (see, e.g., the discussion of [Zum01, §6.2]), *changes in stability/Morse index associated with passage of a single eigenvalue through $\lambda = 0$ are necessarily associated with bifurcation/nonuniqueness.*

7 Numerical investigations

7.1 Feasible set

For our numerical studies, we rescale (2.1) through the following change of coordinates, $\rho = \rho_0 \bar{\rho}$, $u = u_0 \bar{u}$, $e = u_0^2 \bar{e}$, $t = \frac{\bar{t}}{u_0}$, $\bar{\alpha} := \frac{\alpha}{\rho_0 u_0}$, $\bar{\nu} := \frac{\nu}{\rho_0 u_0}$, which allows us to always fix

$\rho_0 = u_0 = 1$. We note that the assumption concerning the ratio of viscosities for simple gasses still holds under this change of coordinates, $16\bar{\nu} = \bar{\alpha}(27\Gamma+12)$. Hereafter, we drop the bar notation. To map out the feasible set, we solve the profile equation (2.6) (with $u_0 = 1$) as an initial value problem on the interval $[0, 1]$ with initial conditions $(u, e)(0) = (1, e_0)$ for various values of the integration constants c_1, c_2 . We center the map about the integration constants corresponding to the fixed point, $c_1 = -1 - \Gamma e_0$, $c_2 = -\frac{1}{2} - (1 + \Gamma)e_0$. We tested our feasibility set independently using a constant step-size RKF four to fifth order scheme we coded by hand, and using standard suite software in MatLab. For improved accuracy, for the large scale study we use MatLab's *ode15s* routine which is an adaptive step, stiff ODE solver. The solver warnings alert us to finite blowup, and testing a solution tells us whether or not u and e remain positive throughout the unit interval. In Figure 1, we plot some examples of the feasible set. Note that the feasible set is unbounded (see Lemma 4.3).

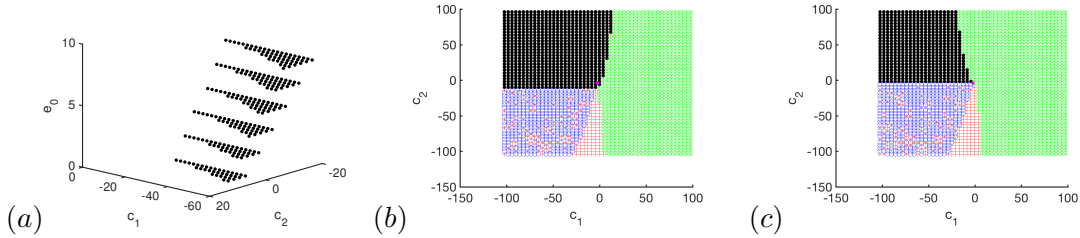


Figure 1: (a) Plot of the feasible set as e_0 varies when $\Gamma = 1$, $\alpha = 0.1$, and $\nu = 0.244$. (b) Plot of the feasible set with black dots, the set where u goes negative on $[0, 1]$ with blue circles, the set where e goes negative on $[0, 1]$ with green stars, and the set where there is finite time blowup on $[0, 1]$ with red + signs for $\alpha = 2$, $\nu = 3.75$, $\Gamma = 2/3$, $e_0 = 2$. (c) Plot of the feasible set with black dots, the set where u goes negative on $[0, 1]$ with blue circles, the set where e goes negative on $[0, 1]$ with green stars, and the set where there is finite time blowup on $[0, 1]$ with red + signs for $\alpha = 0.2$, $\nu = 1$, $\Gamma = 2/3$, $e_0 = 2$. A bold magenta dot marks the constant solution on plots (b) and (c).

We ran large batch jobs to test if the following parameters lie in the feasibility set,

$$(\Gamma, \alpha, e_0, \Delta c_1, \Delta c_2) \in \{2/3, 2/5, 1\} \times \text{lin}(0.1, 2, 10) \times \text{lin}(0.001, 10, 30) \\ \times \text{lin}(-50, 50, 50) \times \text{lin}(-50, 50, 50),$$

where $\text{lin}(a, b, c)$ indicates the set containing c evenly spaced points in the interval $[a, b]$, $\nu = \frac{\alpha(27\Gamma+12)}{16}$, and $c_1 = -1 - \Gamma e_0 + \Delta c_1$, $c_2 = -\frac{1}{2} - (1 + \Gamma)e_0 + \Delta c_2$.

7.2 Evans function computations

To compute the Evans function, we use the the flux coordinates described in Section 3.1 of [BHLZ18a], which is equivalent to computing with coordinates (ρ, u, e, u', e') as described

in Section 6. To improve numerical conditioning of the computation, we evaluate the Evans function wronskian at $x = 1/2$ with ODE solutions given in the definition of the Evans function initialized at $x = 0$ with $\{(0, 1, 0, 0, 0)^T, (0, 0, 1, 0, 0)^T\}$ and at $x = 1$ with $\{(1, 0, 0, 0, 0)^T, (0, 1, 0, 0, 0)^T, (0, 0, 1, 0, 0)^T\}$ to recover, as given by Abel's Theorem, a non-vanishing multiple of the Evans function. We also use the method of continuous orthogonalization [HZ06] without the radial equation using Drury's method [Dru80] in order to compute the ODE solution, which resolves computational challenges due to differing growth modes. To verify the correctness of our code, we computed $D(0)$ with the radial equation by initializing the ODE solutions at $x = 0$ only and evolving them to take the determinant at $x = 1$ with the initializing basis there, and checked that this matched the value of $D(0)$ computed with the definition given in (6.4). We further note that our code, which is part of STABLAB [BHLZ], is well tested by this point; for example see [BHLZ15, BJN⁺17, BLZ11].

7.3 Winding number computations

To test for the existence of unstable eigenvalues, we compute the Evans function on a contour consisting of the boundary ∂S of the set $S := \{z \in B(0, 100) : \Re(z) \geq 0\}$. We use the functionality built into STABLAB [BHLZ] that adaptively chooses the mesh along ∂S so that the relative error between any two consecutive points on the image of ∂S under the Evans function, C_S , varies by no more than 0.2. We then compute the winding number of C_S , which is the number of eigenvalues of (6.1) inside S . In Figure 2, we demonstrate the profile and corresponding Evans function computation for representative parameters.

We computed the Evans function on the contour ∂S for the parameters, if they are in the feasible set, given by

$$(\Gamma, \alpha, e_0, \Delta c_1, \Delta c_2) \in \{2/3, 2/5, 1\} \times \text{lin}(0.1, 2, 10) \times \text{lin}(0.001, 10, 30) \\ \times \text{lin}(-50, 50, 50) \times \text{lin}(-50, 50, 50),$$

where $\text{lin}(a, b, c)$ indicates the set containing c evenly spaced points in the interval $[a, b]$, $\nu = \frac{\alpha(27\Gamma+12)}{16}$, $c_1 = -1 - \Gamma e_0 + \Delta c_1$, and $c_2 = -\frac{1}{2} - (1 + \Gamma)e_0 + \Delta c_2$. In all, we computed the Evans function on 670,926 contours, and in all cases found the winding number to be zero. To complete these computations took the equivalent of approximately 83.8 computation days on a desktop with 11 duo cores.

7.4 Global uniqueness/stability index

For the parameters in the feasible set described in Section 7.1, we computed the Evans function at the origin, $D(0)$. We found that the smallest value of $D(0)$ for the computed parameters is 4.19e-4. Thus, $D(0)$ appears not to vanish on the feasible set, confirming global uniqueness. See Figure 3 for a demonstration of how $D(0)$ varies as c_1 and c_2 vary in the feasible set.

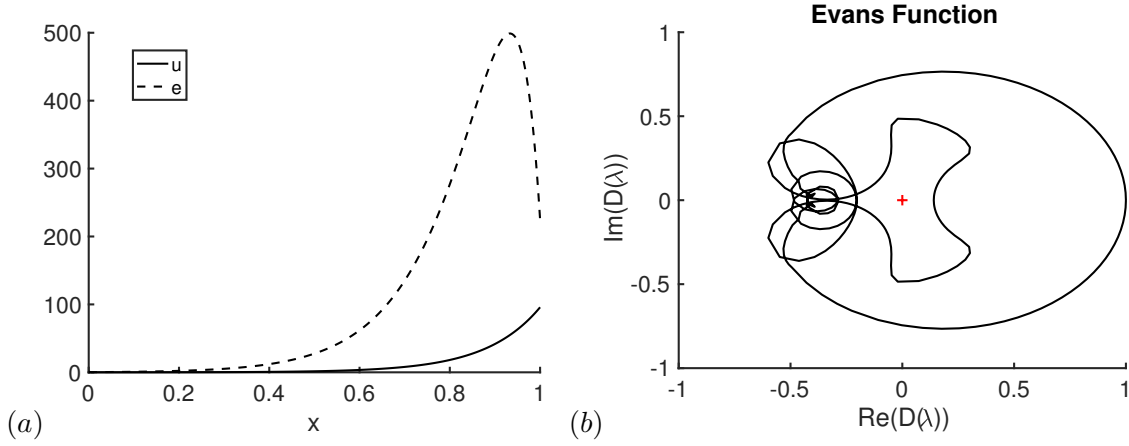


Figure 2: For the parameters $\alpha = 0.1$, $\Gamma = 1$, $\nu = 0.2438$, $e_0 = 0.001$, $c_1 = -18.35$, and $c_2 = 0.5184$, we plot (a) the boundary layer profile, and (b) the image $S := \{z \in B(0, 100) : \Re(z) \geq 0\}$ under the Evans function. The winding number is zero indicating spectral stability of the boundary layer profile.

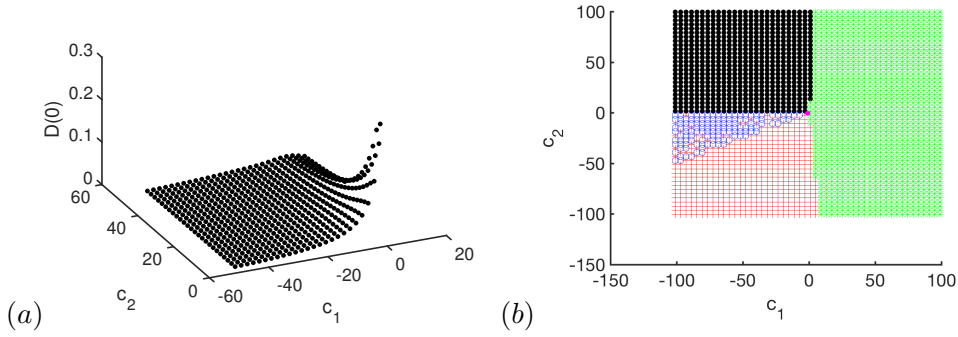


Figure 3: In these figures, $\alpha = 0.7\bar{3}$, $\Gamma = 2/3$, $\nu = 1.375$, and $e_0 = 0.001$. (a) Plot of $D(0)$ against c_1 and c_2 . (b) Plot of the feasible set corresponding to Figure (a) with black dots, the set where u goes negative on $[0, 1]$ with blue circles, the set where e goes negative on $[0, 1]$ with green stars, and the set where there is finite time blowup on $[0, 1]$ with red + signs.

8 A numerical counterexample

We now consider equations (2.1) subject to the equation of state $\bar{e}(\tau, S) = \frac{e^S}{\tau} + S + \frac{\tau^2}{2}$ considered in [BFZ15], where τ corresponds to specific volume and S corresponds to entropy. Specific density is given by $\rho = \frac{1}{\tau}$, and $T = \bar{e}_S = \frac{e^S}{\tau} + 1$, so $e^S = \frac{T-1}{\rho}$, or

$$(8.1) \quad S = \hat{S}(\rho, T) = \ln \left(\frac{T-1}{\rho} \right).$$

From this, we obtain

$$(8.2) \quad \begin{aligned} p &= \hat{p}(\rho, T) = -\bar{e}_\tau = \rho(T-1) - \frac{1}{\rho}, \\ e &= \hat{e}(\rho, T) = T-1 + \ln \left(\frac{T-1}{\rho} \right) + \frac{1}{2}\rho^2, \end{aligned}$$

closing the system, together with the energy relation $E = e + \frac{1}{2}u^2$, in terms of variables (ρ, u, T) , $T > 1$. Alternatively, inverting the relation $e = \hat{e}(T, \rho)$ using $\hat{e}_T > 0$ for $T > 1$, we may consider it as implicitly determining a system in the usual variables (ρ, u, e) , with $e > 0$. This is the system referred to as the *local model* in [BFZ15]. Notably, the function $\eta := -\hat{S}(\rho, T)$, with \hat{S} as in (8.1) considered as a function of the conservative variables $(\rho, \rho u, E)$ is a *convex entropy for system* (2.1) in the sense of Appendix A.4; see [BFZ15].

In [BFZ15] it was shown that the local model considered on the whole line has unstable shock waves for parameters for which the inviscid system has stable waves. Here, we demonstrate that the local model considered on a finite interval has parameters for which uniqueness of solutions fails, and also other, nearby parameters for which a Hopf-bifurcation occurs.

These results are guided by the general principles of Appendix A.6 relating spectra of standing shocks on the whole line to spectra of pieces thereof, considered as solutions on a finite interval. The first relevant principle is that spectra on the interval are, for $\Re \lambda \geq 0$ and $\lambda \neq 0$ given in the limit as interval length goes to infinity- equivalently, as viscosity goes to zero- by the direct sum of spectra on the whole line together with spectra of constant boundary layers on the half-line with data corresponding to that on the left (resp. right) endpoint of the interval. This implies that strict instability on the whole line implies strict instability on the interval (Proposition A.10), with associated stability transition as amplitude is increased from a constant steady solution to an unstable one.⁵

The second principle is that in the same large interval length/small viscosity standing-shock limit, the stability index does not vanish (Proposition A.11), or equivalently $D(0) \neq 0$. Thus, if a homotopy is taken from stable constant solutions to unstable standing shock solutions, entirely within the class of standing shocks with sufficiently large interval/small viscosity, then the associated stability transition cannot correspond to a simple crossing of an eigenvalue through the origin $\lambda = 0$, as $D(0) \neq 0$, and must therefore involve the crossing of one or more pairs of complex conjugate roots, i.e., a Hopf-type scenario.

⁵Stability of constant steady solutions for entropy systems is shown in Theorem A.9), Appendix A.4.

On the other hand, the first cited principle implies that two of these roots must be near the pair of roots at the origin of the whole-line shock as it undergoes transition to instability: one “translational” eigenvalue fixed at $\lambda = 0$ and the crossing eigenvalue corresponding to instability. Thus, we have the picture of a Hopf bifurcation with very nearby roots, i.e., with associated time-period going to infinity, a quite delicate scenario. This makes numerical verification somewhat sensitive; however, it also aids us in finding a more standard bifurcation in the form of a single crossing eigenvalue through $\lambda = 0$, as we are able to find by playing with the left and right boundaries of the interval for a given, sufficiently large-amplitude standing shock on the whole line.

8.1 Nonuniqueness

8.1.1 Abstract bifurcation result

We first demonstrate a bifurcation implying nonuniqueness. Namely, we show for the local model with finite boundaries that $D(0)$ changes sign as x_L and x_R vary, where the local model is posed on the finite interval given by $[x_L, x_R]$; see Figure 6 (a)-(c). Defining by $c_*(x_L, x_R)$ the value of c corresponding to the shock profile on $[x_L, x_R]$, define the map

$$\Phi(c; x_L, x_R) := \psi(c_*(x_L, x_R) + c; x_L, x_R) - \psi(c_*(x_L, x_R); x_L, x_R),$$

where $\psi(x; x_L, x_R)$ is the solution map ψ associated with the interval $[x_L, x_R]$. Then $\Phi(0; x_L, x_R) \equiv 0$, reflecting the fact that the shock profile restricted to $[x_L, x_R]$ solves its own data. Existence of additional roots $c \neq 0$ for some x_L, x_R implies nonuniqueness for the same data. Nonuniqueness is then a consequence of the following abstract bifurcation result in the spirit of Proposition 5.1.

Proposition 8.1. *Let $\Phi(c; p) : \mathbb{R}^m \times \mathbb{R}$ satisfy $\Phi(0; p) \equiv 0$. If $\gamma := \det(d\Phi(0; p))$ changes sign as p crosses a particular bifurcation value $p = p_*$, then $\Phi(\cdot; p)$ has a nontrivial root $c \neq 0$ for p arbitrarily close to p_* .*

Proof. Arguing by contradiction, suppose that $c = 0$ is the unique root of $\Phi(c; p) = 0$ for p in a neighborhood of p_* . Thus, Φ does not vanish on the boundary of a small ball $B(0, r)$, hence the topological degree of $\Phi(\cdot; p)$ is independent of p . However, at p for which $\det(d\Phi(0; p)) > 0$, the degree is by the assumed uniqueness of roots equal to $+1$, while at points p for which $\det(d\Phi(0; p)) < 0$, the degree is -1 , a contradiction. \square

To show non-uniqueness, we first solve for the profile corresponding to the whole-line shock. Then we take the piece of that solution on $[x_L, x_R]$ as the profile for the finite boundary problem posed on the same interval. The computations showing non-uniqueness are relatively difficult. In the following discussion, $S_- := \lim_{x \rightarrow -\infty} S(x)$, is the left end state value of entropy in the whole-line shock wave solution of the local model. To solve for the profile, we fix the parameters $\alpha = \kappa = 1$ and take $S_- = 1$. From the Rankine-Hugoniot conditions, we obtain the other parameters. We then use MatLab’s `bvp5c` boundary value solver to obtain the whole-line viscous shock solution. Next, we use continuation with 30

evenly spaced steps in S_- to obtain the solution at $S_- = -5$. That is, we change the parameter S_- by a small amount and solve for the other parameters given by the Rankine-Hugoniot conditions, then use the profile solution corresponding to the previous value of S_- as an initial guess in `bvp5c` to solve for the profile for the new parameters. In solving for the whole-line profile, we use the `profile_flux` module built into STABLAB which adaptively increases the spatial domain $[-L, L]$, $L \gg 1$, until the profile converges to the fixed-point end states corresponding the shock at $x = \pm\infty$ to within requested tolerance, which was $1e-6$ in this study. To compute the Evans function, we used the same procedure as described in Section 7.2, except that we evaluated the Wronskian to obtain the Evans function at $x = 0$ instead of $(x_L + x_R)/2$, and we used “pseudo-Lagrangian coordinates” as described in [BHLZ18b] to reduce winding in our winding number studies without changing the zeros of the Evans function. In the Evans function computations, we used `ode15s` in MatLab with the requested relative and absolute error tolerance set to $1e-10$ and $1e-12$ respectively.

8.1.2 Multiple solutions

We next find numerically an explicit example of two distinct profiles solving the same data. To demonstrate abstract non-uniqueness of profile solutions, our general strategy was to take a piece of the whole-line shock for an unstable wave in the local model, and truncate it to a finite interval. By varying the boundary on the left of this finite interval, we were able to observe a change of sign of the Evans function evaluated at the origin, $D(0)$, indicating non-uniqueness of solutions occurs. Fixing the interval to be $[x_L, x_R] = [-33.17, 2.9]$, we then computed the Evans function at the origin for profiles with varying c_1 and c_2 to find regions in c_1 and c_2 for which $D(0)$ has opposite sign; see Figure 4(a)-(b). Explicit parameter pairs (\hat{c}_1, \hat{c}_2) and $(\tilde{c}_1, \tilde{c}_2)$ that correspond to two distinct profiles solving the same data must lie in regions for which $D(0)$ has opposite sign. We note that the null clines of $D(0)$ shown in Figure 4 are nearly parallel, which is expected since these profiles are nearly translationally invariant. Indeed, it is the small eigenvalue corresponding to translational invariance of the whole line profile that makes these computations delicate.

A nice way to find two parameter pairs corresponding to two distinct profiles solving the same data is to look at null clines of the mappings $M_1(c_1, c_2) := u_L(c_1, c_2) - u_L^*(c_1^*, c_2^*)$ and $M_2(c_1, c_2) := T_L(c_1, c_2) - T_L^*(c_1^*, c_2^*)$. Here (c_1^*, c_2^*) are fixed constants of integration that correspond to the whole line shock, which constants of integration we find by solving for them in the Rankine-Hugoniot equation. The other terms used in defining M_1 and M_2 , that is $u_L(c_1, c_2)$ and $T_L(c_1, c_2)$, are the components of the profiles evaluated at $x = x_L$. We note that these profiles have the same data at $x = x_R$ as the profile corresponding to (c_1^*, c_2^*) . In particular, $u_R(c_1, c_2) = u_R(c_1^*, c_2^*)$ and $T_R(c_1, c_2) = T_R(c_1^*, c_2^*)$. The levels sets of M_1 and M_2 intersect in two locations, which we name (\hat{c}_1, \hat{c}_2) and $(\tilde{c}_1, \tilde{c}_2)$, along the same curves indicating that these constants of integration correspond to two distinct profiles solving the same data; see Figure 4 (c)-(d). We plot the profiles corresponding to (\hat{c}_1, \hat{c}_2) and $(\tilde{c}_1, \tilde{c}_2)$ in Figures 5(a)-(b). We note that there is approximately a 20% difference between the lower curves, in terms of the ratio of the ≈ 0.2 maximum difference between the two curves to the ≈ 1.0 total variation of each curve, far more than can be attributed to numerical error.

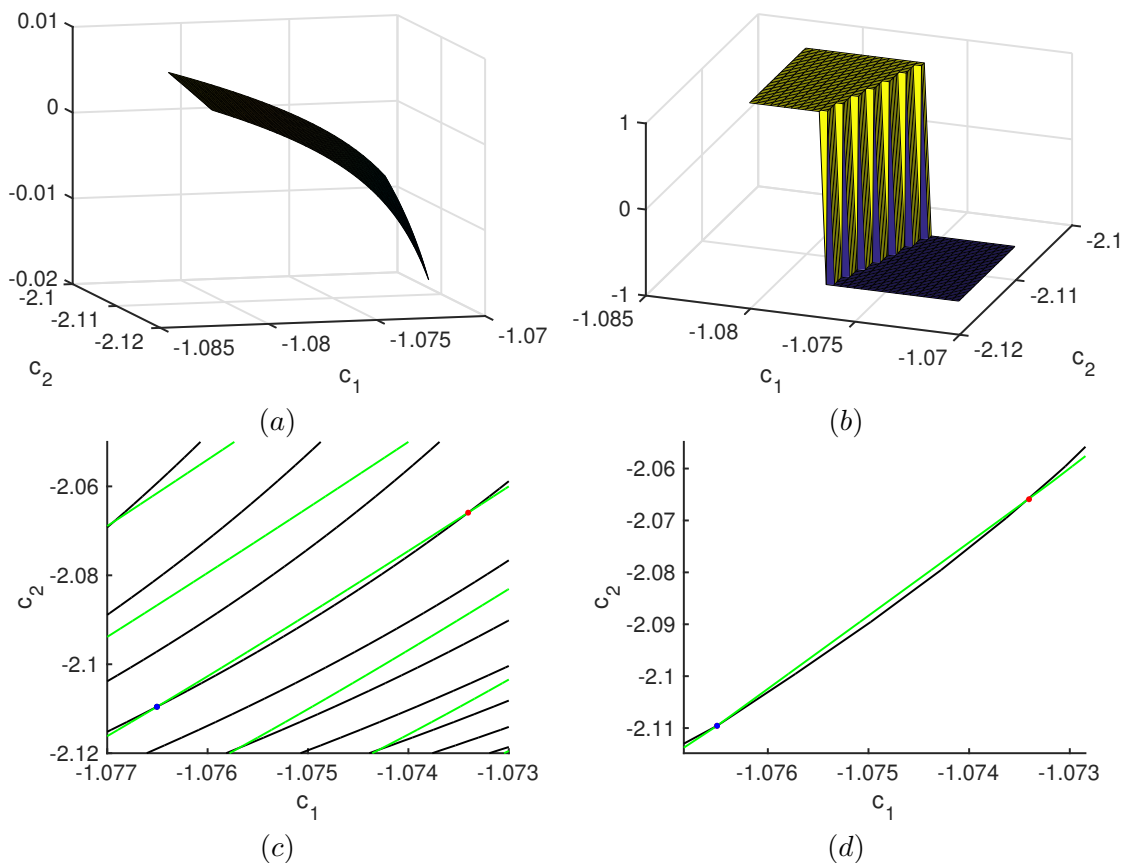


Figure 4: Figures (a)-(b) demonstrate that $D(0)$ changes sign as c_1 and c_2 vary. Figures (c)-(d) indicate that there are distinct profiles that solve the same data since there are nullclines of M_1 and M_2 that intersect twice. (a) Plot of $D(0)$ against c_1 and c_2 . (b) Plot of $\text{sign}(D(0))$ against c_1 and c_2 . (c) Plot of the null clines of M_1 and M_2 . Dots indicate intersections of the null clines. (d) Plot of only the two intersecting null clines seen in (c).

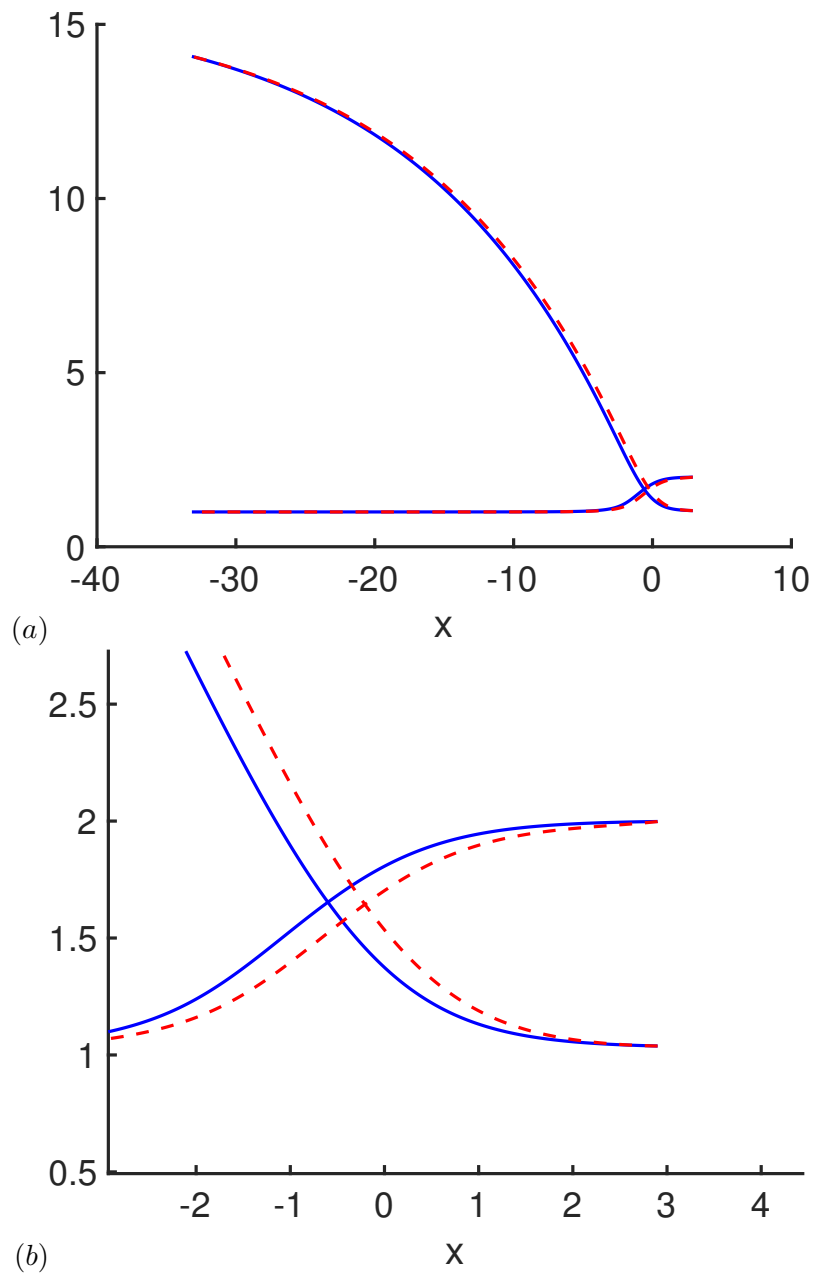


Figure 5: (a) Plot of the two profiles, solving the same data, against x . The solid blue curves and dashed red curves correspond to the profiles with c_1 and c_2 values plotted as dots with the same colors in Figure 4(c)-(d). (b) Zoomed in picture of (a) near $x = x_R$.

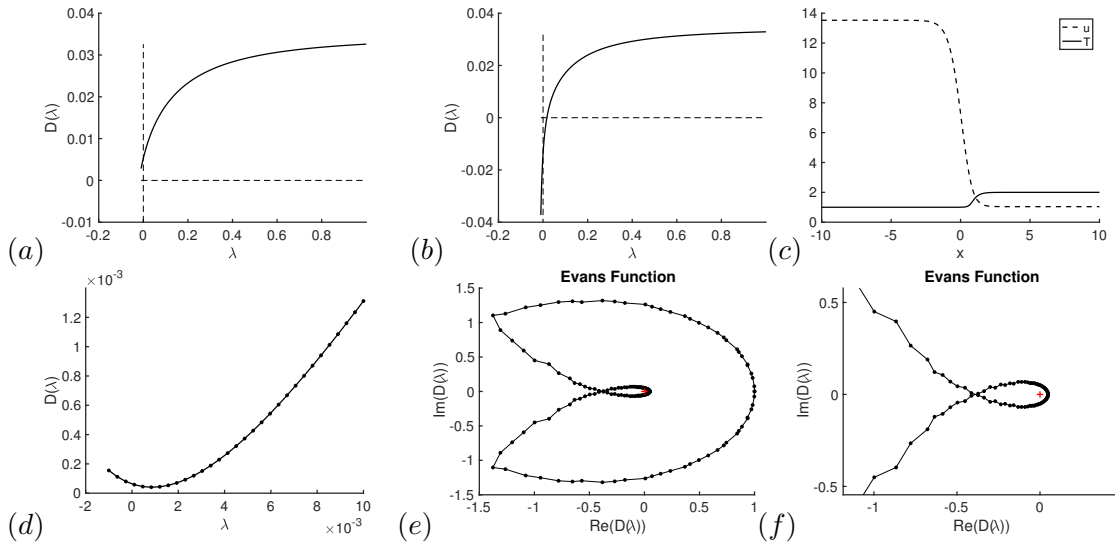


Figure 6: The parameters of the local model in this figure are $\mu = 0.5$, $\kappa = 1$, $T_- \approx 1.001$, $T_+ = 2$, $\rho_- \approx 0.0769$, $\rho_+ = 1$, $u_+ \approx 1.041$, $u_- \approx 13.53$, and $M \approx 1.041$. (a) Plot of $D(\lambda)$ against λ where $x_L = -0.5$ and $x_R = 2.15$. (b) Plot of $D(\lambda)$ against λ where $x_L = -0.7$ and $x_R = 3.01$. (c) Plot of the whole-line viscous shock profile. (d) Plot of $D(\lambda)$ against λ where $x_L = -4.3$ and $x_R = 4.3$. (e) Plot of $\Im(D(\lambda))$ against $\Re(D(\lambda))$ where $x_L = -4.3$, $x_R = 4.3$, and $D(\cdot)$ is evaluated on $\partial(\{z \in B(0, 1e-3) : \Re(z) \geq 0\})$. (f) Zoomed in view of (e).

8.2 Hopf bifurcation

Using the same shock parameters in the local model that we used to show a bifurcation implying non-uniqueness, but with different choices of left and right boundary, we can show also the existence of a Hopf-bifurcation. When the finite boundaries are $x_L = -4.3$, $x_R = 4.3$, and the whole-line shock is truncated to $[x_L, x_R]$, the Evans function evaluated on the real line segment $[0, 10^{-3}]$ has no zeros, whereas the image of the Evans function evaluated along $\partial(\{z \in B(0, 1e - 3) : \Re(z) \geq 0\})$ has winding number of two. Thus, there is a complex conjugate pair of eigenvalues with non-zero imaginary part, indicating that a Hopf-bifurcation occurs; see Figure 6 (d)-(e).

A General systems

In this appendix, we augment our results for polytropic gas dynamics with a series of partial results for general systems, some of which are used in the main body of the paper. Consider steady solutions of general viscous conservation laws:

$$(A.1) \quad \partial_t U + f(U)_x = (B(U)U_x)_x, \quad 0 < x < 1, \quad t > 0,$$

where

$$U = \begin{pmatrix} U_I \\ U_{II} \end{pmatrix} \in \mathbb{R}^r \times \mathbb{R}^{n-r}, \quad B = \begin{pmatrix} 0 & 0 \\ 0 & B_{22} \end{pmatrix}, \quad B_{22} \in M_{n-r}(\mathbb{R}),$$

with the boundary conditions

$$(A.2) \quad U(0) = U_0 = \begin{pmatrix} U_{0I} \\ U_{0II} \end{pmatrix} \quad \text{and} \quad U_{II}(1) = U_{1II}.$$

We make the following assumptions:

(H0) f and B are smooth.

(H1) $B_{22}(U) + B_{22}(U)^t > 0$ for any U .

(H2) for $f = (f_I, f_{II})$, the partial derivative $(df_I)_I(U)$ has positive eigenvalues for any U .

Condition **(H1)** corresponds to the strict parabolicity of (A.1)⁶. Condition **(H2)** means that the flow moves from the left to the right (which explains the boundary condition for U_I at $x = 0$). In the following, we define $A(U) = df(U)$ and

$$A = \begin{pmatrix} A_{11} & A_{12} \\ A_{21} & A_{22} \end{pmatrix}, \quad A_{11} \in M_r(\mathbb{R}).$$

⁶note that $B_{22}(U)$ is necessary invertible.

A.1 The linear case

We assume in this part that df and B are both constant. We have the following proposition.

Proposition A.1. *If df and B are both constant and conditions **(H0)**-**(H2)** are satisfied, Problem (A.1) has a unique steady state that satisfies the boundary condition (A.2) if and only if*

$$(A.3) \quad \sigma(B_{22}^{-1}(A_{22} - A_{21}A_{11}^{-1}A_{12})) \cap 2i\pi\mathbb{Z} \setminus \{0\} = \emptyset.$$

Remark A.1. *Condition (A.3) is a compatibility condition between the parabolic and the hyperbolic part. A similar condition was assumed for the study of quasilinear noncharacteristic boundary layers (on the half-line) in, for instance, [Mét03, Lemma 5.1.3] or [Mét04]. For example, the following system does not satisfy Condition (A.3)*

$$U_t + \begin{pmatrix} 0 & 2\pi \\ -2\pi & 0 \end{pmatrix} U_x = U_{xx}, \quad 0 < x < 1,$$

and any constant state \hat{U} must satisfy $\hat{U}(0) = \hat{U}(1)$.

Proof. We can rewrite the problem as

$$\begin{cases} A_{11}U'_I + A_{12}U'_{II} = 0, \\ A_{21}U'_I + A_{22}U'_{II} = B_{22}U''_{II}. \end{cases}$$

Then, integrating, we get

$$\begin{cases} A_{11}U_I + A_{12}U_{II} = C_1, \\ A_{21}U_I + A_{22}U_{II} + C_2 = B_{22}U'_{II} \end{cases}$$

where $C_1 = A_{11}U_{I0} + A_{12}U_{II0}$ and C_2 is a constant that has to be determined. Then, since A_{11} is invertible, we obtain

$$\begin{cases} U_I = A_{11}^{-1}C_1 - A_{11}^{-1}A_{12}U_{II}, \\ U'_{II} = B_{22}^{-1}(A_{22} - A_{21}A_{11}^{-1}A_{12})U_{II} + B_{22}^{-1}(C_2 + A_{21}A_{11}^{-1}C_1). \end{cases}$$

Denoting $\tilde{A} = B_{22}^{-1}(A_{22} - A_{21}A_{11}^{-1}A_{12})$ and $\tilde{C} = B_{22}^{-1}(C_2 + A_{21}A_{11}^{-1}C_1)$, we solve

$$\begin{cases} U'_{II} = \tilde{A}U_{II} + \tilde{C} \\ U_{II}(0) = U_{II0}. \end{cases}$$

We decompose \tilde{A} as $\tilde{A} = P^{-1} \begin{pmatrix} F_1 & 0 \\ 0 & F_2 \end{pmatrix} P$ where P and F_2 are invertible and F_1 is strictly upper triangular. We get that

$$U_{II}(1) = e^{\tilde{A}}U_{II}(0) + P^{-1} \begin{pmatrix} \int_0^1 e^{sF_1} ds & 0 \\ 0 & F_2^{-1}(e^{F_2} - I) \end{pmatrix} P\tilde{C}.$$

Thus, we see that the map $C_2 \rightarrow U_{II}(1)$ is invertible if and only if $\sigma(\tilde{A}) \cap 2i\pi\mathbb{Z} \setminus \{0\} = \emptyset$. \square

A.2 Almost constant steady states

We next study the existence of steady states for system (A.1)-(A.2) under the spectral assumption (A.3). We seek solutions \hat{U} of

$$(A.4) \quad (f(\hat{U}))_x = \left(B(\hat{U})\hat{U}_x \right)_x, \quad 0 < x < 1, \quad U(0) = U_0, \quad U_{II}(1) = U_{1II}.$$

Similarly as for gas dynamics, for U_0 fixed, we define the map

$$\Phi : (U_{1II}, C_2) \rightarrow U_{II}(1) - U_{1II} \in \mathbb{R}^{n-r},$$

for $(U_{1II}, C_2) \in \mathbb{R}^{n-r} \times \mathbb{R}^{n-r}$ such that the maximal solution U of the ODE

$$(A.5) \quad B_{22}(U)U'_{II} = f_{II}(U) - f_{II}(U_0) + B_{22}(U_0)C_2, \quad U_{II}(0) = U_{0II}, \quad f_I(U) = f_I(U_0)$$

is defined on $[0, 1]$. Thus, profiles are equivalent to roots C_2 of $\Phi(U_{1II}, \cdot)$.

Theorem A.2. *Let $U_0 \in \mathbb{R}^n$ and assume conditions **(H0)**-**(H2)** are satisfied. Assume that Condition (A.3) is satisfied for $A = df(U_0)$ and $B = B(U_0)$. There exists $\delta > 0$ and $\varepsilon > 0$ such that for any U_{1II} with $|U_{0II} - U_{1II}| \leq \delta$, there exists a unique solution \hat{U} of (A.4) satisfying*

$$\left| \hat{U}'_{II}(0) \right| \leq \varepsilon.$$

Moreover, the solution is nondegenerate: i.e., corresponds to a nondegenerate root of Φ .

Remark A.3. *We do not claim that for U_{1II} close enough to U_{0II} , there exists a unique solution of (A.4). The previous theorem only gives a local uniqueness.*

Proof. Let us fix $U_0 \in \mathbb{R}^n$. First, we notice that for $U_{1II} = U_{0II}$, $\hat{U} \equiv U_0$ is a solution of (A.4). Then, by continuous dependence on parameters on the ODE, **(H2)** and the implicit function theorem on the constraint $f_I(U_I, U_{II}) = 0$, for (U_{1II}, C_2) close enough to $(U_{0II}, 0)$, one can express U_I as a function of U_{II} and the maximal solution U of (A.5) is defined on $[0, 1]$. Therefore, we can define the map Φ on a neighborhood V of $(U_{0II}, 0)$ in $\mathbb{R}^{n-r} \times \mathbb{R}^{n-r}$. The function Φ is \mathcal{C}^1 on this domain and $\Phi(U_{0II}, 0) = 0$. Then, for any $D \in \mathbb{R}^{n-r}$, $d_2\Phi(U_0, 0) \cdot D = V_{II}(1)$, V_{II} solving

$$B_{22}(U_0)V'_{II} = (A_{22} - A_{21}A_{11}^{-1}A_{12})(U_0)V_{II} + C_2 + (A_{21}A_{11}^{-1})(U_0)C_1, \quad V_{II}(0) = 0,$$

with $C_1 = A_{11}(U_0)U_{I0} + A_{12}(U_0)U_{II0}$. As in the proof of Proposition A.1, we can solve this ODE and, using Condition (A.3), we obtain that $d_2\phi(U_0, 0)$ is invertible. The result then follows from the implicit function theorem, as does nondegeneracy. \square

A.3 Symmetrizable systems

The spectral condition (A.3) is satisfied for many physical systems. We first have the following technical lemma.

Lemma A.4. *If \tilde{A} is symmetric and $\tilde{B} + \tilde{B}^t > 0$, then $\sigma(\tilde{B}^{-1}\tilde{A}) \cap i\mathbb{R} \setminus \{0\} \subset \{0\}$.*

Proof. If $\tilde{B}v = i\tau\tilde{A}v$ for $\tau \neq 0$, we get

$$2i\tau\langle v, \tilde{A}v \rangle = \langle v, (\tilde{B} + \tilde{B}^t)v \rangle + \langle v, (\tilde{B} - \tilde{B}^t)v \rangle.$$

and since $\tilde{B} + \tilde{B}^t > 0$, $v = 0$. □

We recall that (A.1) is said to be symmetrizable if:

(H3) there exists a smooth map $S : U \in \mathbb{R}^n \mapsto S(U)$ such that, for any $U \in \mathbb{R}^n$, $S(U)$ is a definite positive symmetric matrix, $S(U) = \begin{pmatrix} S_{11}(U) & 0 \\ 0 & S_{22}(U) \end{pmatrix}$, $S(U)A(U)$ is symmetric and $S_{22}(U)B_{22}(U) + (S_{22}(U)B_{22}(U))^t > 0$.

Then we have the following useful Lemma.

Lemma A.5. *Under assumption (H3), $\sigma(B_{22}^{-1}(A_{22} - A_{21}A_{11}^{-1}A_{12})) \cap i\mathbb{R} \subset \{0\}$.*

Proof. We note first that by assumption $S_{22}A_{21} = (S_{11}A_{12})^t$. Then we write

$$B_{22}^{-1}(A_{22} - A_{21}A_{11}^{-1}A_{12}) = (S_{22}B_{22})^{-1}(S_{22}A_{22} - (S_{11}A_{12})^t(S_{11}A_{11})^{-1}S_{11}A_{12})$$

and the result follows from the previous lemma. □

Corollary A.6. *For symmetrizable systems satisfying Conditions (H0)-(H3), almost constant solutions of almost constant data exist and are locally unique, nondegenerate, and spectrally stable.*

Remark A.7. *Note that contrary to the whole line situation (see for instance [Kaw83, KS88, Zum04]) we do not assume a Kawashima's genuine coupling condition. The main reason behind is that a steady state \hat{U} of a purely hyperbolic system on a interval under assumptions (H0), (H2), (H3) is stable. Even better, any solution of Problem (A.1)-(A.2) initially close enough to \hat{U} is equal to \hat{U} after a finite time.*

Proof. Existence, local uniqueness, and nondegeneracy are immediate consequences of Theorem A.2 and Lemma A.5. For spectral stability of a steady state \hat{U} , one can easily adapt [MZ19, Prop. 3.2] and prove that the spectrum of the linearized operator only contains eigenvalues. We then consider the eigenvalue problem

$$\lambda V + (A(\hat{U})V)_x = \left(B(\hat{U})V_x + dB(\hat{U})V\hat{U}_x \right)_x, \quad V(0) = 0, \quad V_{II}(1) = 0.$$

If $\hat{U} \equiv U_0$, one can check that (note that Conditions (H2)-(H3) give $S_{11}A_{11} > 0$ ⁷)

$$\Re(\lambda) (S(U_0)V, V)_{L^2(0,1)} + (S_{22}(U_0)B_{22}(U_0)V_{IIx}, V_{IIx})_{L^2(0,1)} + \frac{1}{2} |\sqrt{S_{11}(U_0)A_{11}(U_0)}V_I(1)|^2 = 0$$

⁷since $A_{11}(U)$ is symmetric for the inner product associated to $S_{11}(U)$.

so that U_0 is spectrally stable. Furthermore, for almost constant steady states (meaning \hat{U}_x small enough), using an appropriate Goodman-type estimate and Poincaré inequality, one can check that

$$\Re(\lambda) \left(\varphi S(\hat{U})V, V \right)_{L^2(0,1)} \leq -\alpha (V, V)_{L^2(0,1)}$$

for some $\alpha > 0$ and $\varphi > 0$ such that

$$\varphi' S(\hat{U})A(\hat{U}) + \varphi \left((S(\hat{U}))_x A(\hat{U}) - S(\hat{U})(A(\hat{U}))_x \right) < 0.$$

Then \hat{U} is also spectrally stable. See [MZ19, Section 3] for similar computations in the isentropic gas dynamic case. \square

Remark A.8. *Using the same kind of energy estimates, one can also prove the nonlinear stability of a steady state. See [MZ19, Section 6] for similar considerations in the isentropic gas dynamic case.*

A.4 Systems with convex entropy

A system (A.1) is said to have a convex entropy [Kaw83, KS88] if it has an entropy/entropy flux pair $(\eta, q) : \mathbb{R}^n \rightarrow \mathbb{R}^2$ such that

$$d^2\eta > 0, \quad d\eta dq = df, \quad d^2\eta B + (d^2\eta B)^t \geq 0, \quad \text{with equality only on } \ker B.$$

It is a theorem of [KS88] that existence of a convex entropy implies symmetrizability, i.e., reducibility by coordinate change to a system satisfying **(H3)** thus, we may deduce local uniqueness information for systems with a convex entropy already by reference to Corollary A.6.

Arguing directly, we obtain the following much stronger, *global*, uniqueness result.

Theorem A.9. *For systems (A.1)-(A.2) with a global convex entropy and satisfying Conditions **(H0)**-**(H3)**, solutions of (A.4) for constant data $U_{0II} = U_{1II}$ are globally unique, nondegenerate (full rank), and spectrally stable, consisting exclusively of constant states.*

Proof. Following [Lax73], we obtain by multiplying (A.1) by $d\eta$ and using $d\eta df = dq$ the equation $\eta_t + q_x = d\eta(BU_x)_x = (d\eta BU_x)_x - \langle U_x, d^2\eta BU_x \rangle$. Since $d^2\eta B + (d^2\eta B)^t \geq 0$, we have $\langle U_x, d^2\eta BU_x \rangle \geq 0$, hence, integrating the steady equation from $x = 0$ to $x = 1$, we obtain

$$(A.6) \quad (q(U) - d\eta(U)B(U)U')|_0^1 \leq 0,$$

with equality if and only if $\langle U', d^2\eta BU' \rangle \equiv 0$, or equivalently $U'_{II} \equiv 0$.

On the other hand, integrating the U_I equation, we have $f_I(U) \equiv \text{constant}$, whence, by **(H2)** and the implicit function theorem, $U_I(0) = U_I(1)$, and so $U(0) = U(1)$. Thus, $q(U)|_0^1$ vanishes in (A.6). At the same time, by addition of an arbitrary linear function, we may take η without loss of generality to satisfy $d\eta(U(0)) = d\eta(U(1)) = 0$, whence the entire

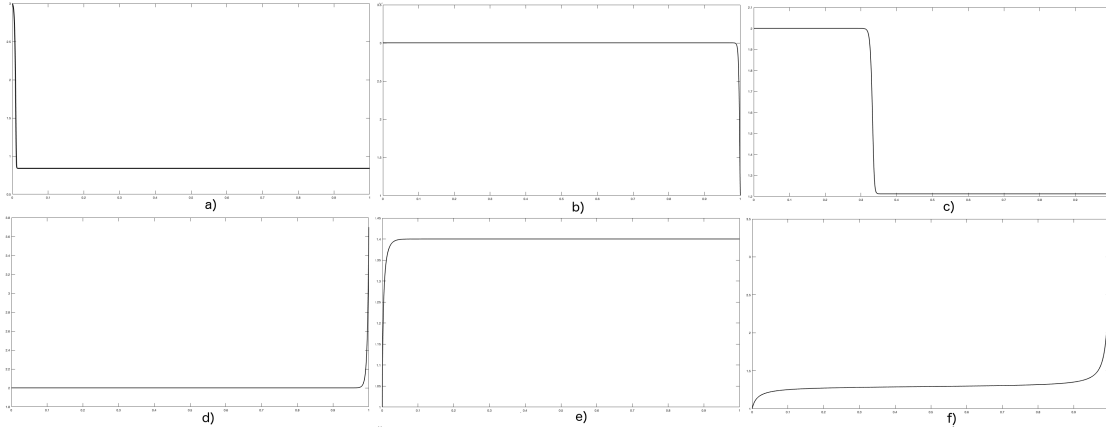


Figure 7: Steady solutions of the Navier-Stokes isentropic equations on $(0, 1)$ for a viscosity $\nu = 0.01$. Panels a) and b) depict left and right compressive boundary layers, c) an interior shock, and d) and e) left and right expansive boundary layers, each connecting to nondegenerate rest states of the steady profile ODE, hence exponentially convergent. Panel f) depicts a double boundary layer (expansive) consisting of left and right degenerate (hence non-exponentially convergent) boundary layers meeting at a characteristic middle state.

lefthand side of (A.6) vanishes. Thus, we must have $U'_{II} \equiv 0$ and $U_{II} \equiv \text{constant}$. Applying (H2) and the implicit function theorem once more to solve for U_I as a function of U_{II} and f_I , we find that $U_I \equiv \text{constant}$ as well, yielding global uniqueness of the constant solution. Nondegeneracy and spectral stability then follow by Corollary A.6. \square

A.5 Small-viscosity/large interval asymptotics

In either the vanishing-viscosity limit, or the large-interval limit $[0, X]$, $X \rightarrow +\infty$ after rescaling back to the unit interval $[0, 1]$, we are led to consider in place of (A.1)

$$(A.7) \quad \partial_t U + f(U)_x = \varepsilon (B(U)U_x)_x, \quad 0 < x < 1,$$

with $\varepsilon = \frac{1}{X}$, $\varepsilon \rightarrow 0^+$, and the steady profile equation is

$$(A.8) \quad f(U)' = \varepsilon (B(U)U')'.$$

Formally setting $\varepsilon = 0$ in (A.8), we obtain $f(U) \equiv \text{constant}$, or $U \equiv \text{constant}$ on smooth portions, separated by standing shock and boundary layers. This indicates a rich “zoo” of possible steady solution structures. Some examples from the isentropic gas dynamics case are displayed in Figure 7.

A.5.1 Feasible configurations

It is readily deduced that the limiting configurations depicted in Figure 7 are in fact the only possibilities for the isentropic case. For, $\rho u \equiv \text{constant}$ imposes $\rho, u > 0$ throughout the

limiting pattern, whence all states have either one or two positive characteristics $\alpha = u \pm c$, where c is sound speed. This in turn implies, by general results of [MZ03] that, as rest points of the scalar steady profile ODE, they are attractors or repellers, respectively. A nontrivial nondegenerate boundary layer at the left endpoint $x = 0$ must terminate at $x = 0^+$ at a rest point, which must therefore be an attractor; at the right endpoint, $x = 1^-$ a repeller. Interior shocks must connect a repeller on the left with a saddle on the right. It follows that nontrivial boundary layers and interior shocks cannot coexist, but occur only separately. Moreover, there can occur at most one nondegenerate boundary layer, either at the left or the right endpoint. The final possibility completing our zoo of possible configurations is a double boundary layer configuration, for which the end point must necessarily be degenerate, corresponding to a “sonic”, or “characteristic” point where $u = c$. Shocks or boundary layers connecting to a nondegenerate rest point decay exponentially; those connecting to a degenerate rest point decay algebraically. For further discussion of boundary layer structure for the compressible Navier-Stokes equations, see, e.g., [SZ01, GMWZ05].

For the nonisentropic case, we again have $\rho, u > 0$, imposing in this instance that state have either two or three positive characteristics $\alpha = u - c, u, u + c$; as rest points of the steady profile equation, these correspond to saddle points or repellers, respectively. Similar analysis to the above yields again that left boundary layers and shocks cannot coincide; however, there is the new possibility of patterns consisting of a left boundary layer plus a right boundary layer, or an interior shock plus a right boundary layer, as nontrivial right boundary layers may connect to either repellers or saddles in the nonisentropic case.

A.5.2 Rigorous asymptotics

A very interesting open problem would be to carry out the zero-viscosity limit rigorously, in preparation for the more complicated dynamics of the 2d shock tube problem. One might hope also to understand the spectra of such wave patterns as the approximate direct sum of the spectra of component layers, as would follow, for example, by the methods of [Zum10, Zum11] if the components layers remained appropriately spatially separated in the limit. A first apparently nontrivial step, of interest in its own right, is to show for given boundary data existence and uniqueness of feasible limiting patterns as described in Section A.5.1.

A.6 The standing shock limit

A simple case in which the zero-viscosity limit can be completely carried out is that of the “standing-shock limit” generalizing the study of [Zum10] in the case of the half-line. This consists of the study of a stationary viscous n -shock $\hat{U}^\varepsilon(x) = \bar{U}(\frac{1}{\varepsilon}(x - \frac{1}{2}))$ of (A.7), solving (A.8) for all $\varepsilon > 0$, with respect to its “own” boundary conditions, i.e.

$$U_0 = \hat{U}^\varepsilon(0), \quad U_1^{II} = \hat{U}^\varepsilon(1).$$

We consider this for the general class of system (A.1),(A.2) under assumptions **(H0)**-**(H3)** plus the additional assumption used in [Zum10]

(H4) the eigenvalues of $df(U_0)$ and $df(U_1)$ are nonzero.⁸

Converting by $x \rightarrow \frac{x}{\varepsilon}$ to the large-interval limit and following the arguments of [Zum10] word for word, we find that, away from $\lambda = 0$, the spectra of the linearized operator about $\hat{U}^X(x) := \hat{U}^\varepsilon(\varepsilon x)$ on $\Re\lambda \geq 0$ approaches, as $\varepsilon = \frac{1}{X} \rightarrow 0^+$, the direct sum of the spectra of the viscous shock \bar{U} as a solution on the whole line plus the spectra of the constant boundary layers on the half-lines $(0, +\infty)$ and $(-\infty, 1)$ determined by the values of \hat{U}^ε at 0 and 1 with the boundary conditions for the steady problem at $x = 0$ and $x = 1$. As the latter constant layers have been shown to be spectrally stable [GMWZ05], this implies that the spectra of \hat{U}^X converges away from $\lambda = 0$ to that of \bar{U} as $X \rightarrow \infty$. Rescaling, we find that, outside $B(0, c\varepsilon^{-1})$, any $c > 0$, the spectra of \hat{U}^ε are well-approximately by ε^{-1} times the spectra of \bar{U} . We record this observation as the following proposition cited in Section 8.

Proposition A.10 (Spectral decomposition). *For viscous n -shock solutions \bar{U} of systems (A.1) satisfying (H0)–(H4), the corresponding standing-shock family \bar{U}^ε contains no spectra $\Re\lambda \geq 0$ outside a ball $B(0, c\varepsilon^{-1})$ for $\varepsilon > 0$ sufficiently small, for any choice of $c > 0$, if and only if \bar{U} is spectrally stable, i.e., has no spectra $\Re\lambda \geq 0$ with $\lambda \neq 0$. In particular, if \bar{U} is spectrally unstable, then \bar{U}^ε is spectrally unstable for ε sufficiently small.*

Proposition A.10 gives no information about the corresponding stability index and the uniqueness or the nonuniqueness. However, this is provided definitively by the following result.

Proposition A.11 (Nonvanishing of the stability index). *For viscous n -shock solutions \bar{U} of systems (A.1) satisfying (H0)–(H4), the Evans function D^ε associated with the corresponding standing-shock family \bar{U}^ε satisfies $D^\varepsilon(0) \neq 0$ for $\varepsilon > 0$ sufficiently small.*

Proof. We only sketch the proof, which belongs more to the circle of ideas in [Zum10] than those of the present paper. We first write the eigenvalue system in “flux” variables (u_{II}, F) as

$$(A.9) \quad \begin{aligned} U'_{II} &= B_{22}(U)^{-1}(F_{II} + A_{11}U_I), \\ F' &= \lambda U, \end{aligned}$$

where $F := B(\hat{U})U' - AU$ and $U_I = A_{11}^{-1}(F_I + A_{12}U_{II})$. This yields for $\lambda = 0$ in the second equation the simple dynamics $F \equiv \text{constant}$.

Next, we observe that the Evans function may be written equivalently as

$$D^\varepsilon(\lambda) = \det \begin{pmatrix} U_{II}^1 & \cdots & U_{II}^r & 0 \\ F^1 & \cdots & F^r & I_n \end{pmatrix} \Big|_{x=1},$$

⁸By (H3) the eigenvalues of $df(U)$ are real and semi-simple since $df(U)$ is symmetric for the inner product associated to $S(U)$.

where $\begin{pmatrix} U_{II}^j \\ F^j \end{pmatrix}$, $j = 1, \dots, r$ denote the solutions of (A.9) with initial conditions

$$(A.10) \quad \begin{pmatrix} U_{II}^1 & \cdots & U_{II}^r \\ F^1 & \cdots & F^r \end{pmatrix} (0) = \begin{pmatrix} 0 \\ B(0) \begin{pmatrix} 0 \\ I_r \end{pmatrix} \end{pmatrix}$$

at $x = 0$. In turn, we may view this as a Wronskian

$$(A.11) \quad D^\varepsilon(\lambda) = \det \begin{pmatrix} U_{II}^1 & \cdots & U_{II}^r & U_{II}^{r+1} & \cdots & U_{II}^{n+r} \\ F^1 & \cdots & F^r & F^{r+1} & \cdots & F^{n+r} \end{pmatrix} \Big|_{x=1},$$

where $\begin{pmatrix} U_{II}^j \\ F^j \end{pmatrix}$, $j = r+1, \dots, n+r$ denote the solutions of (A.9) with initial conditions

$$(A.12) \quad \begin{pmatrix} U_{II}^{r+1} & \cdots & U_{II}^{r+n} \\ F^{r+1} & \cdots & F^{r+n} \end{pmatrix} (1) = \begin{pmatrix} 0 \\ I_n \end{pmatrix}$$

at $x = 1$.

By Abel's theorem, vanishing or nonvanishing of the Wronskian (A.11) at $x = 1$ is determined by vanishing or nonvanishing at any $x \in [0, 1]$. By the analysis of [Zum10], we find that, at $x = c$ for any $c > 0$ sufficiently small, the solutions $\begin{pmatrix} U_{II}^j \\ F^j \end{pmatrix}$, $j = 1, \dots, r$ originating from $x = 0$ converge exponentially in $X := 1/\varepsilon$ to the limiting subspace of solutions of (A.9) on the whole line decaying at $x = -\infty$, which may be identified by the property $F \equiv 0$, hence also $\det(U_{II}^1, \dots, U_{II}^r) \neq 0$. Recalling by the simple dynamics for $\lambda = 0$ that

$$(F^{r+1}, \dots, F^{r+n}) \equiv \begin{pmatrix} 0 \\ B(0) \begin{pmatrix} 0 \\ I_r \end{pmatrix} \end{pmatrix},$$

we find that the Wronskian at $x = c$ converges exponentially in $X = \varepsilon^{-1}$ to

$$\det(U_{II}^1, \dots, U_{II}^r) \Big|_{x=c} \neq 0,$$

hence $D^\varepsilon(0) \neq 0$ for $\varepsilon > 0$ sufficiently small. For further details, see [Zum10]. \square

Remark A.12. *The result of Proposition A.11, though proved by similar techniques, stands in striking contrast to the results of [Zum10, SZ01] in the half-line case, where the stability index was seen to change sign as parameters were varied for (full) polytropic gas dynamics.*

References

- [AGJ90] J. Alexander, R. Gardner, and C. Jones. A topological invariant arising in the stability analysis of travelling waves. *J. Reine Angew. Math.*, 410:167–212, 1990.
- [Bat99] G. K. Batchelor. *An introduction to fluid dynamics*. Cambridge Mathematical Library. Cambridge University Press, Cambridge, paperback edition, 1999.
- [BFZ15] B. Barker, H. Freistühler, and K. Zumbrun. Convex entropy, Hopf bifurcation, and viscous and inviscid shock stability. *Arch. Ration. Mech. Anal.*, 217(1):309–372, 2015.
- [BHLZ] B. Barker, J. Humpherys, J. Lytle, and K. Zumbrun. A MATLAB-based numerical library for evans function computation. <https://github.com/nonlinear-waves/stablab.git>.
- [BHLZ15] B. Barker, J. Humpherys, G. Lyng, and K. Zumbrun. Viscous hyperstabilization of detonation waves in one space dimension. *SIAM J. Appl. Math.*, 75(3):885–906, 2015.
- [BHLZ18a] B. Barker, J. Humpherys, G. Lyng, and K. Zumbrun. Balanced flux formulations for multidimensional Evans-function computations for viscous shocks. *Quart. Appl. Math.*, 76(3):531–545, 2018.
- [BHLZ18b] B. Barker, J. Humpherys, G. Lyng, and K. Zumbrun. Euler versus Lagrange: the role of coordinates in practical Evans-function computations. *SIAM J. Appl. Dyn. Syst.*, 17(2):1766–1785, 2018.
- [BHZ10] B. Barker, J. Humpherys, and K. Zumbrun. One-dimensional stability of parallel shock layers in isentropic magnetohydrodynamics. *J. Differential Equations*, 249(9):2175–2213, 2010.
- [BJN⁺17] B. Barker, M. Johnson, P. Noble, M. Rodrigues, and K. Zumbrun. Stability of viscous St. Venant roll waves: from onset to infinite Froude number limit. *J. Nonlinear Sci.*, 27(1):285–342, 2017.
- [BLZ11] B. Barker, M. Lewicka, and K. Zumbrun. Existence and stability of viscoelastic shock profiles. *Arch. Ration. Mech. Anal.*, 200(2):491–532, 2011.
- [Dru80] L. Drury. Numerical solution of Orr-Sommerfeld-type equations. *J. Comput. Phys.*, 37(1):133–139, 1980.
- [GMWZ05] O. Guès, G. Métivier, M. Williams, and K. Zumbrun. Existence and stability of multidimensional shock fronts in the vanishing viscosity limit. *Arch. Ration. Mech. Anal.*, 175(2):151–244, 2005.
- [GZ98] R. A. Gardner and K. Zumbrun. The gap lemma and geometric criteria for instability of viscous shock profiles. *Comm. Pure Appl. Math.*, 51(7):797–855, 1998.
- [HLZ09] J. Humpherys, G. Lyng, and K. Zumbrun. Spectral stability of ideal-gas shock layers. *Arch. Ration. Mech. Anal.*, 194(3):1029–1079, 2009.
- [HLZ17] J. Humpherys, G. Lyng, and K. Zumbrun. Multidimensional stability of large-amplitude Navier-Stokes shocks. *Arch. Ration. Mech. Anal.*, 226(3):923–973, 2017.
- [HZ06] J. Humpherys and K. Zumbrun. An efficient shooting algorithm for Evans function calculations in large systems. *Phys. D*, 220(2):116–126, 2006.
- [Kaw83] S. Kawashima. Systems of a hyperbolic–parabolic composite type, with applications to the equations of magnetohydrodynamics. *Thesis, Kyoto University*, 1983.
- [KK97] J. R. Kweon and R. B. Kellogg. Compressible Navier-Stokes equations in a bounded domain with inflow boundary condition. *SIAM J. Math. Anal.*, 28(1):94–108, 1997.
- [KS88] D. Kawashima and Y. Shizuta. On the normal form of the symmetric hyperbolic-parabolic systems associated with the conservation laws. *Tohoku Math. J. (2)*, 40(3):449–464, 1988.
- [Lax73] P. D. Lax. *Hyperbolic systems of conservation laws and the mathematical theory of shock waves*. Society for Industrial and Applied Mathematics, Philadelphia, Pa., 1973. Conference Board of the Mathematical Sciences Regional Conference Series in Applied Mathematics, No. 11.

- [Lio98] P.-L. Lions. *Mathematical topics in fluid mechanics. Vol. 2*, volume 10 of *Oxford Lecture Series in Mathematics and its Applications*. The Clarendon Press, Oxford University Press, New York, 1998. Compressible models, Oxford Science Publications.
- [Mét03] G. Métivier. *Stability of Small Viscosity Noncharacteristic Boundary Layers*. graduate lectures. 2003.
- [Mét04] G. Métivier. *Small viscosity and boundary layer methods*. Modeling and Simulation in Science, Engineering and Technology. Birkhäuser Boston, Inc., Boston, MA, 2004. Theory, stability analysis, and applications.
- [MZ03] C. Mascia and K. Zumbrun. Pointwise Green function bounds for shock profiles of systems with real viscosity. *Arch. Ration. Mech. Anal.*, 169(3):177–263, 2003.
- [MZ19] B. Melinand and K. Zumbrun. Existence and stability of steady compressible Navier-Stokes solutions on a finite interval with noncharacteristic boundary conditions. *Physica D: Nonlinear Phenomena*, 394:16–25, 2019.
- [Rou01] F. Rousset. Inviscid boundary conditions and stability of viscous boundary layers. *Asymptot. Anal.*, 26(3-4):285–306, 2001.
- [Smo94] J. Smoller. *Shock waves and reaction-diffusion equations*, volume 258 of *Grundlehren der Mathematischen Wissenschaften [Fundamental Principles of Mathematical Sciences]*. Springer-Verlag, New York, second edition, 1994.
- [SZ01] D. Serre and K. Zumbrun. Boundary layer stability in real vanishing viscosity limit. *Comm. Math. Phys.*, 221(2):267–292, 2001.
- [TZ11] B. Texier and K. Zumbrun. Transition to longitudinal instability of detonation waves is generically associated with Hopf bifurcation to time-periodic galloping solutions. *Comm. Math. Phys.*, 302(1):1–51, 2011.
- [ZH02] K. Zumbrun and P. Howard. Errata to: “Pointwise semigroup methods, and stability of viscous shock waves” [Indiana Univ. Math. J. (47) (1998), no. 3, 741–871; MR1665788 (99m:35157)]. *Indiana Univ. Math. J.*, 51(4):1017–1021, 2002.
- [ZS99] K. Zumbrun and D. Serre. Viscous and inviscid stability of multidimensional planar shock fronts. *Indiana Univ. Math. J.*, 48(3):937–992, 1999.
- [Zum01] K. Zumbrun. Multidimensional stability of planar viscous shock waves. In *Advances in the theory of shock waves*, volume 47 of *Progr. Nonlinear Differential Equations Appl.*, pages 307–516. Birkhäuser Boston, Boston, MA, 2001.
- [Zum04] K. Zumbrun. Stability of large-amplitude shock waves of compressible Navier-Stokes equations. In *Handbook of mathematical fluid dynamics. Vol. III*, pages 311–533. North-Holland, Amsterdam, 2004. With an appendix by Helge Kristian Jenssen and Gregory Lyng.
- [Zum10] K. Zumbrun. Stability of noncharacteristic boundary layers in the standing-shock limit. *Trans. Amer. Math. Soc.*, 362(12):6397–6424, 2010.
- [Zum11] K. Zumbrun. Stability of detonation profiles in the ZND limit. *Arch. Ration. Mech. Anal.*, 200(1):141–182, 2011.